Colloquium: Homochirality: Symmetry breaking in systems driven far from equilibrium

Yukio Saito and Hiroyuki Hyuga

Department of Physics, Keio University, 3-14-1 Hiyoshi, Kohoku-ku, Yokohama 223-8522, Japan

(published 2 April 2013)

Subsequent to the discovery of chirality of organic molecules by Pasteur, living organisms have been found to utilize biomolecules of only one handedness. The origin of this homochirality in life still remains unknown. It is believed that homochirality is attained in two stages: the initial creation of a chirality bias and its subsequent amplification to pure chirality. In the last two decades, two novel experiments have established the second stage in different fields: Soai and co-workers achieved the amplification of enantiomeric excess in the production of chiral organic molecules, and Viedma obtained homochirality in the solution growth of sodium chlorate crystals. These experiments are explained by a theory with a nonlinear evolution equation for the chiral order parameter; nonlinear processes in reactions or in crystal growth induce enantiomeric excess amplification, and the recycling of achiral elements ensures homochirality. Recycling drives the system to a state far from equilibrium with a free energy higher than that of the equilibrium state.

DOI: 10.1103/RevModPhys.85.603 PACS numbers: 05.70.Ln, 81.10.Aj, 82.40.−g, 82.39.−k

CONTENTS

I. INTRODUCTION: HOMOCHIRALITY IN LIFE

When a three-dimensional object is not superimposable on its mirror image merely by translation and/or rotation, the object is said to be chiral, a word first used by Kelvin (1904). For instance, our left and right hands are chiral. They are enantiomorphs of each other.

Various chiral substances exist in nature. Quartz crystal is one such substance. It takes two enantiomorphic shapes as schematically shown in Fig. 1(a). Two quartz crystals of different shapes have nearly identical physical properties, except for their response to light. When linearly polarized light passes through quartz, the plane of polarization rotates in the clockwise direction for dextrorotatory *d* quartz, and in the counterclockwise direction for levorotatory *l* quartz. The property was found by Arago (1811, 1858) and is called optical activity.

Other examples of crystals with chirality include sodium chlorate ($NaClO_3$), as shown in Fig. 1(b) (Kipping and Pope, 1898a, 1898b) and tartrates (Pasteur, 1848a, 1848b). However, when these two crystals are dissolved in water, they behave quite differently. The optical activity disappears for $NaClO_3$, while it remains for tartrates. Because a crystal decomposes into its constituent molecules or ions in solution, the above fact indicates that the ions of the $NaClO_3$ molecule have no chirality (they are achiral), whereas some of the ions of tartrate molecules are chiral. This particular case of molecular chirality was first discovered by Pasteur (1848a, 1848b), and thereafter many organic molecules have been found to be chiral. An organic molecule, by definition, contains a carbon atom. When it is surrounded by four molecular residues in a tetragonal stereostructure and the four residues are all different, the tetragonal structure takes one of two configurations that are mutual mirror images, as exemplified by the alanine molecule in Fig. 1(c). Two stereoisomers related by reflection are called enantiomers. In organic chemistry, one enantiomer is called the *R* form (rectus), and the other, the *S* form (sinister); however, for amino acids and sugars, the D/L representation is commonly used.

Amino acids and sugars are vital elements for life. Proteins consist of linear polymer chains of 20 different amino acids,

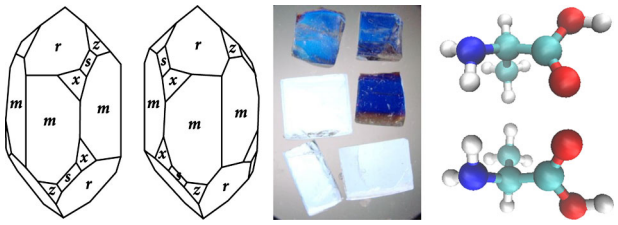

FIG. 1 (color online). Examples of chiral substances. (a) Schematic of *d* and *l* quartz. Adapted from Dana, 1915. (b) Sodium chlorate crystal, courtesy of C. Viedma, and (c) D (upper) and L (lower) alanine. In (b), *d* and *l* crystals are differentiated by their color under polarized light.

and they function everywhere in our body; they form its structure, act as enzymes, and so on. One of the common motifs in the secondary structure of proteins is an α helix where a polymer coils in a right-handed helical conformation. Nucleic acids such as DNA and RNA consist of long chains of nucleotides. Each nucleotide consists of a pentose sugar, a nitrogenous base, and one or more phosphate groups. In DNA two long polymers are entwined in the shape of a double right-handed helix. The double-helix structure is essential for replication and transcription of the genetic information that DNA carries. Genetic codes vary from species to species, and there are differences even within a species. It is remarkable that, in spite of the vast diversity of proteins and nucleic acids, almost all the amino acids found in living organisms are of L type and all sugars are of D type. Thus chiral symmetry is completely broken in life. This symmetry breaking is called *homochirality*.

From the point of view of the energy involved, the two enantiomers are indistinguishable, and they should ideally exist with equal probability. When chiral organic substances are synthesized from achiral substances, we usually obtain a mixture of *R* and *S* enantiomers in a ratio of 50:50 (Pasteur, 1875; Japp, 1898). There is no chirality as a whole, and the mixture is said to be racemic. When $NaClO_3$ crystals are grown from a solution by evaporating water, the ratio of *d* to *l* crystals is 50:50 (Kipping and Pope, 1898a, 1898b). Again, the result is a racemic mixture. By examining the statistics of natural quartz crystals, it is found that they are also racemic (Frondel, 1978; Klabunovskii and Thiemann, 2000). The question arises as to why organic molecules in living organisms are homochiral. Pasteur in 1860 stated that homochirality is the demarcating difference between living organisms and artificial products (or dead matter) (Pasteur, 1875; Japp, 1898). More than a century later, the problem of homochirality in living organisms has remained unsolved. The origin of this problem is believed to be connected to the origin of life (Bada, 1995). Homochirality in elementary building blocks such as sugars and amino acids might be necessary for the formation of regular and stable structures of DNA and proteins. However, there is no preference for one enantiomer over the other. For instance, an all-D amino acid enzyme, artificially synthesized, was shown to have the expected specificity for mirror image substrates (Milton, Milton, and Kent, 1992).

It is speculated that homochirality in living organisms is established in two stages (Bonner, 1991): (1) an initial creation of chiral bias, and (2) a subsequent amplification of the small bias to the chiral pure state. The chirality bias is measured by enantiomeric excess (EE), defined as the ratio of the concentration difference of the two enantiomers to the total concentration; EE is unity in a homochiral state.

For creation of the initial chiral bias in biomolecules, various possibilities have been proposed (Japp, 1898; Bonner, 1991; Feringa and van Delden, 1999). Because of the discrete nature of molecules, there is always a statistical fluctuation such that one type of enantiomer is slightly in excess compared to the other (Pearson, 1898a, 1898b; Siegel, 1998; Lente, 2006, 2007). The Earth's rotation around its axis may affect the initial symmetry breaking. Kovacs, Keszthelyi, and Goldanskii (1981) simulated rotation by stirring polymerizing D and L amino acid solutions clockwise and counterclockwise, but they observed no stereoselectivity that exceeds the fluctuation level. Asymmetric adsorption on quartz surfaces affects their biomolecular chirality (Bonner *et al.*, 1974). However, since the chirality of natural quartz crystals is random (Frondel, 1978), the biomolecular chirality on Earth is expected to be random as well (Bonner, 1991). Circularly polarized light (CPL) has intrinsic chirality and is capable of stereoselective interactions with chiral molecules. In fact, CPL has been shown to destroy one enantiomer preferentially (Kuhn and Braun, 1929; Kuhn and Knopf, 1930; Feringa and van Delden, 1999), and this asymmetric photolysis enhances EE (Balavoine, Moradopour, and Kagan, 1974; Kagan, Balvoine, and Moradpour, 1974). However, it is questionable whether sufficiently intense CPL is available from the Sun (Bonner, 1991). When parity conservation is discovered to be violated (Lee and Yang, 1956; Wu *et al.*, 1957), the electroweak interactions are expected to induce an energy difference between two enantiomers, and thus probably lead to a state with a finite EE (Yamagata, 1966). Several research groups have evaluated the energy difference by *ab initio* calculation (Mason and Tranter, 1985; Bakasov, Ha, and Quack, 1998), but the results are controversial and its effect on chirality selection remains an open question (Bonner, 2000; Wesendrup *et al.*, 2003). Apart from the terrestrial origin, the idea of extraterrestrial origin has also been proposed, since amino acids on meteorites are found to have an excess of L amino acids (Cronin and Pizzarello, 1997; Engel and Macko, 1997). The origin of this bias is supposed to be rapidly rotating neutron stars which emit strong CPL (Bailey *et al.*, 1998). Even if all of these proposals are taken into account, the initial difference in the amounts of enantiomers (the EE) is much too small to achieve homochirality (Bonner, 1991; Avalos *et al.*, 2000). For that, one needs mechanisms to amplify the initial small quantity of EE. Our primary focus in the remainder of the paper is this amplification process.

The second stage is not simply the amplification of the EE; it is also necessary to maintain a steady and stable homochiral state. The first simple model for homochirality was proposed by Frank (1953). His model consisted of a linear (or first-order) autocatalytic production of enantiomers with mutual destruction in an open system. If two enantiomers of different chiralities form an inactive product and flow away from the system, only the initial majority enantiomer eventually remains. Subsequently, linear autocatalysis

continues to produce the remaining enantiomer. Following this classical work by Frank, many theoretical models were proposed (Calvin, 1969; Kondepudi and Nelson, 1983; Girard and Kagan, 1998; Plasson, Bersini, and Commeyras, 2004), and these models have been summarized in many reviews (Goldanskii and Kuz'min, 1988; Avetisov and Goldanskii, 1996; Kondepudi and Asakura, 2001; Plasson *et al.*, 2007).

It is only recently that real experimental systems have been discovered which actually show EE amplification or homochirality. In this review we mainly focus on these recent experiments performed in the last two decades and also on related theoretical studies. The first experimental system is a chemical reaction system discovered by Soai *et al.* (1995). The system showed EE amplification for the first time, as shown in Fig. 2; its origin is attributed to nonlinear (or higher-order) autocatalysis. By iterating the reaction, the EE is enhanced to more than 99% (Sato, Urabe *et al.*, 2003). It was theoretically shown later that if a recycling process of an achiral reactant is included, the system can achieve a homochiral steady state (Saito and Hyuga, 2004).

The second system is the growth from solution of $NaClO_3$ crystals as obtained by Viedma (2005), and he achieved homochirality. The system itself has been studied since the 19th century, and we summarize these studies in a later section. The novelty of Viedma's experiment was that he prepared a solution with crystallites of both enantiomorphs and added glass beads. When such a solution is stirred, the glass beads grind the crystallites into small fragments. If the initial system has a small enantiomorphic bias, all the crystallites show the same handedness as the initial majority after a few hours, as shown in Fig. 3; homochirality is accomplished by grinding. Later, the grinding method was successfully extended to many systems of crystal growth from solution. In order to elucidate the phenomena involved, various theories have been proposed (Uwaha, 2004, 2008; Saito and Hyuga, 2005a, 2010, 2011; Noorduin, Meeks *et al.*, 2008). Among them, simulation studies of lattice-gas models have identified a novel mechanism to achieve homochirality (Saito and Hyuga, 2010, 2011).

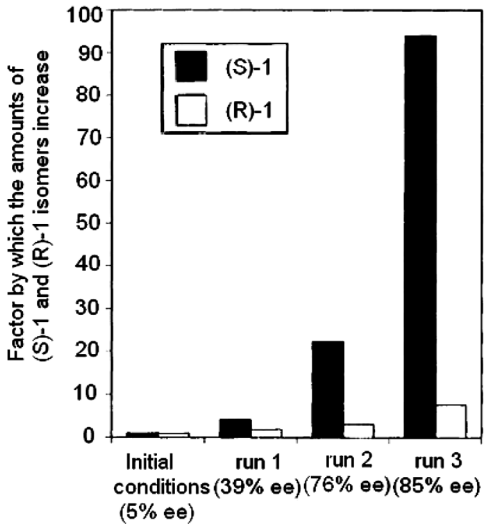

FIG. 2. Enantiomeric amplification during consecutive autocatalytic Soai reaction. Adapted from Soai *et al.*, 1995.

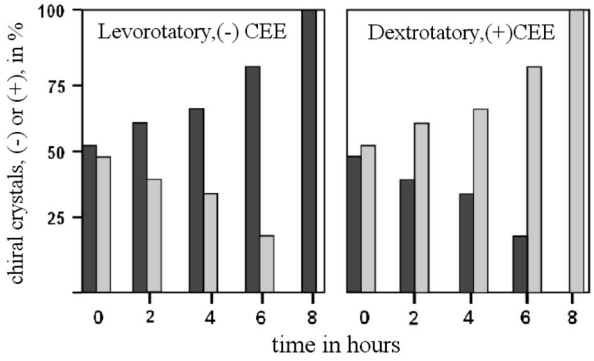

FIG. 3. Temporal evolution of the ratio of chiral crystals. Initial majority dominates eventually in the short time of 8 h. Adapted from Viedma, 2005.

Theoretical studies of the two different systems, chemical reaction and crystal growth, have shown that the chiral order parameter ϕ follows essentially the same time evolution in both cases (Saito and Hyuga, 2004, 2010). The time evolution is nonlinear in ϕ with a coefficient depending on the density of the achiral parent material. The recently proposed activation, polymerization, epimerization, and depolymerization (APED) model (Plasson, Bersini, and Commeyras, 2004; Brandenburg, Lehto, and Lehto, 2007) for homochirality in life is also found to reduce to the same type of nonlinear evolution equation. Thus, the homochirality reported in three different fields, crystal growth, organic chemistry, and biochemistry, is described by a universal nonlinear time evolution. The specific features of the different systems lie in the coefficients of the evolution equation.

II. FRANK MODEL

Before describing recent discoveries, we first summarize the very basic theory of homochirality derived by Frank (1953). He proposed a chemical reaction model in which an achiral reactant A turns into chiral products, R or S molecules. The system is open such that the achiral reactant A is supplied from outside and its concentration a is kept fixed. If the reactant A comes into contact with a chiral R (or S) molecule, A turns into R (or S) with a rate constant k_1,

$$k_1\colon A + R \rightarrow 2R, \qquad A + S \rightarrow 2S. \tag{2.1}$$

The production process is linearly autocatalytic (or of the first order). When the two opposite enantiomers R and S come into contact, they annihilate with a rate constant μ:

$$\mu\colon R + S \rightarrow 0. \tag{2.2}$$

Frank called the process "mutual antagonism." The two different enantiomers do not necessarily annihilate each other, but may form a heterodimer RS, which leaves the system by evaporation or sedimentation (Girard and Kagan, 1998).

If there is only a mutual destruction μ without autocatalytic production, i.e., $k_1 = 0$, the asymptotic state is trivially homochiral such that the initial majority survives whereas the initial minority is eliminated. With linear autocatalysis with a finite k_1, the remaining molecules of the initial majority steadily multiply.

The reaction is quantified by rate equations. We denote the concentrations of the R and S enantiomers as r and s, respectively. The time variation with linear autocatalysis and mutual antagonism is described by the following rate equations:

$$\frac{dr}{dt} = k_1 ra - \mu rs, \qquad \frac{ds}{dt} = k_1 sa - \mu rs. \tag{2.3}$$

Here the concentration of the achiral reactant a is kept constant since it is assumed to be supplied externally in an open system.

The system relaxes asymptotically to fixed points (or steady states) determined by $dr/dt = ds/dt = 0$. From Eq. (2.3), one finds a racemic fixed point

$$r^* = s^* = k_1 a/\mu. \tag{2.4}$$

However, it is unstable, since the concentration difference diverges exponentially as $r - s = (r_0 - s_0)e^{k_1 at}$, where r_0 and s_0 denote the initial values of r and s, respectively. The system approaches the racemic fixed point (r^*, s^*) only if the initial state is completely achiral, i.e., $r_0 = s_0$. If there is initially a slight chiral bias ($r_0 \neq s_0$), the difference $r - s$ increases and the majority enantiomer dominates over the minority. By solving the time evolution equation (2.3) numerically, the flow is obtained in the r-s phase space, as shown in Fig. 4(a). The system asymptotically approaches homochiral states $(r, s) = (0, \infty)$ or $(\infty, 0)$.

The process of chiral symmetry breaking is easy to observe in terms of the chiral order parameter

$$\phi = \frac{r - s}{r + s}, \tag{2.5}$$

or EE defined as $|\phi|$. From the time evolution equations (2.3), we can derive the following equation for the order parameter $\phi(t)$:

$$\frac{d\phi}{dt} = \frac{\mu(r + s)}{2}\phi(1 - \phi^2). \tag{2.6}$$

Here the coefficient of the mutual antagonism μ appears explicitly, thereby indicating that without mutual antagonism ($\mu = 0$) there is no EE variation. The rate constant k_1 used for linear autocatalysis is absent in Eq. (2.6). Its effect is implicitly expressed in the coefficient through the time-dependent variables $r(t) + s(t)$. Equation (2.6) appears similar to the time-dependent Ginzburg-Landau (TDGL) equation that is well known in the field of phase transition. However, there is a significant difference from the TDGL equation in the sense that the coefficient $\mu(r + s)$ is time dependent. Equation (2.6) is not closed in itself; we transformed the original evolution equations (2.3) into the one for the asymmetric variable ϕ [Eq. (2.6)] and for the symmetric one $(r + s)$, which is not written explicitly.

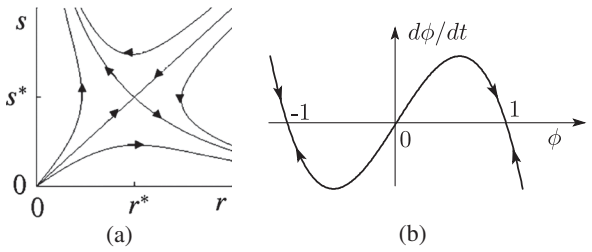

FIG. 4. Time evolution of the Frank model. (a) Flow in r-s phase space. Adapted from Frank, 1953. (b) The relation between the chiral order parameter ϕ and its variation $d\phi/dt$.

From Eq. (2.6), we can discuss the possibility of spontaneous chiral symmetry breaking. Since the coefficient $\mu(r + s)/2$ is non-negative, the growth rate $d\phi/dt$ behaves as a function of ϕ, as shown in Fig. 4(b), at any instant of time. It is clear that there are three fixed points for ϕ that are independent of time, i.e., the racemic state ($\phi = 0$) and the two homochiral states ($\phi = \pm 1$). If the initial value of the order parameter ϕ_0 is positive but small, the growth rate $d\phi/dt$ is positive and ϕ should gradually approach the homochiral point $\phi = 1$. If $-1 < \phi_0 < 0$, then $d\phi/dt < 0$ and ϕ decreases to the other homochiral point $\phi = -1$. Thus, the racemic state $\phi = 0$ is unstable, and the homochiral states $\phi = \pm 1$ are stable as long as the coefficient $\mu(r + s)/2$ is positive. Symmetry breaking requires the presence of a finite amount of the chiral products $r + s$ and mutual antagonism at any time.

Modified Frank model. A modification to the Frank model was proposed by Kondepudi and Nelson (1983, 1985), and we briefly summarize it in the present terminology. In the Frank model, chiral enantiomers are produced only by the linearly autocatalytic process. In the modified model, they may also be produced directly and spontaneously from an achiral reactant. Reverse reactions to the spontaneous and autocatalytic processes are also included in the modified model. Then it is shown that chiral symmetry breaking is possible only when the concentration of an achiral reactant a is larger than the critical value a_c, which is a function of the reaction rate coefficients (Kondepudi and Nelson, 1983).

When a small chiral bias factor g is introduced into the rate coefficients, the chiral order parameter ϕ is shown to evolve near the critical point a_c as

$$\frac{d\phi}{dt} = -A\phi^3 + B(a - a_c)\phi + Cg + \eta(t), \tag{2.7}$$

where A, B, and C are positive coefficients determined by the reaction rates, and $\eta(t)$ is a random force representing thermal fluctuation (Kondepudi and Nelson, 1985). By numerical solution of this Langevin equation while increasing the control parameter $a(t)$ through the critical value a_c, the chiral order parameter ϕ is found to relax to the value of the chiral state preferred by the bias g (Kondepudi and Nelson, 1985). This result implies the possibility that a small chiral bias introduced by the electroweak interactions leads to chiral symmetry breaking, if the small bias is coupled with an EE amplification process (Yamagata, 1966).

The difficulty with the above scenario is that no such chemical system with EE amplification was actually known until the Soai reaction was discovered (Soai *et al.*, 1995). In Secs. III and IV, we review recent discoveries of actual systems which show homochirality and EE amplification.

III. HOMOCHIRALITY IN CRYSTAL GROWTH

Homochirality in crystal growth has been achieved with various materials. The earliest successful attempt was

reported by Viedma (2005) who used an inorganic molecule, sodium chlorate. After his success, the same method was applied to organic molecules, and homochiral crystals have been successfully produced (Noorduin, Izumi *et al.*, 2008; Noorduin, Meeks *et al.*, 2008; Viedma *et al.*, 2008). In the following sections, we briefly summarize the history of the growth from solution of sodium chlorate, and then describe homochiral crystal growth of organic materials. Subsequently, we present a theoretical analysis of the homochirality process with simulations (Saito and Hyuga, 2008, 2009, 2010, 2011).

A. Experiments with $NaClO_3$

The spontaneous homochirality of sodium chlorate crystals has been pursued for a long time. The sodium chlorate molecule $NaClO_3$ itself is achiral, but it crystallizes into two enantiomorphs, its *d* and *l* forms, in the chiral space group $P2_13$ (Abrahams and Bernstein, 1977).

1. Evaporation (Kipping and Pope)

In the experiment by Kipping and Pope (1898a, 1898b), the solution of sodium chlorate was not rotated, and as the water evaporated many crystallites were nucleated spontaneously and grew. The experiment was repeated many times. For each sample, numbers of *d* and *l* crystallites were counted, and the ratio of *d* crystals among them was tabulated. In a later study, Kondepudi, Kaufman, and Singh (1990) repeated similar experiments and examined the results thoroughly. They found that the average crystalline enantiomeric excess (CEE) was essentially zero, since the frequency distribution of the CEE was centered at the racemic point with CEE = 0, as shown in Fig. 5(a).

Kipping *et al.* also studied the effect of chiral impurities. They added D glucose to the sodium chlorate solution and found that the quantity of the *d* crystal decreased such that the ratio of the *d* to *l* crystals was 30:70. This fact clearly indicates the interaction between molecular and crystal chirality.

The spontaneous formation of crystal nuclei in the solution is called primary nucleation. In addition to the experiments on primary nucleation in a supersaturated solution, Kipping *et al.* also studied secondary nucleation process; they crushed a crystallite of sodium chlorate into small fragments and added them to a saturated sodium chlorate solution. The added fragments acted as secondary nucleation centers, and all the 290 crystals grown turned out to have the same chirality. This indicates that the final crystallites were all descendants of the initially fragmented crystallite and no primary nucleation occurred during crystal growth.

2. Stirring (Kondepudi)

Kondepudi, Kaufman, and Singh (1990) grew sodium chlorate crystals from a supersaturated solution by evaporation. During the growth, the solution was stirred with a magnetic stirrer. After the completion of crystallization, only one enantiomorph of the crystallites was observed. They repeated the crystallization experiments several times; the average CEE was zero, but its frequency distribution showed two sharp peaks at the homochiral states, as shown in Fig. 5(b).

In order to understand the mechanism of the development of homochirality, Kondepudi *et al.* monitored the degree of supersaturation during crystal growth. Because of the evaporation of water, supersaturation increased at an early stage. When the first primary nucleation occurred, the supersaturation dropped drastically, and it never again reached the level necessary for further primary nucleation.

McBride and Carter (1991) filmed the solidification process, and they found that a magnetic stir bar stroked the first nucleated crystal, thereby breaking the crystal into small fragments. They acted as secondary nucleation centers and subsequently grew into new crystals. In such a case of secondary nucleation, the supersaturation drops greatly and subsequent primary nucleation is suppressed. Kondepudi *et al.* (1993) quantitatively confirmed the scenario by a theoretical analysis with stochastic kinetic equations. Since only the descendants of the first parent crystal remained, they accordingly had the same chirality (McBride and Carter, 1991; Kondepudi *et al.*, 1993; Martin, Tharrington, and Wu, 1996). Instead of contact with a stir bar, convection in the fluid has also been proposed to induce secondary nucleation (Buhse *et al.*, 2000; Cartwright *et al.*, 2004). Chiral symmetry breaking induced by the secondary nucleation is observed in crystallization of other compounds from solution with stirring, such as 1, 1′-binaphthyl (Kondepudi, Laudadio, and Asakura, 1999), and it is summarized by Kondepudi and Asakura (2001).

3. Grinding (Viedma)

Viedma (2005) placed both *d* and *l* crystallites of sodium chlorate in water as the solvent. Some of the crystallites

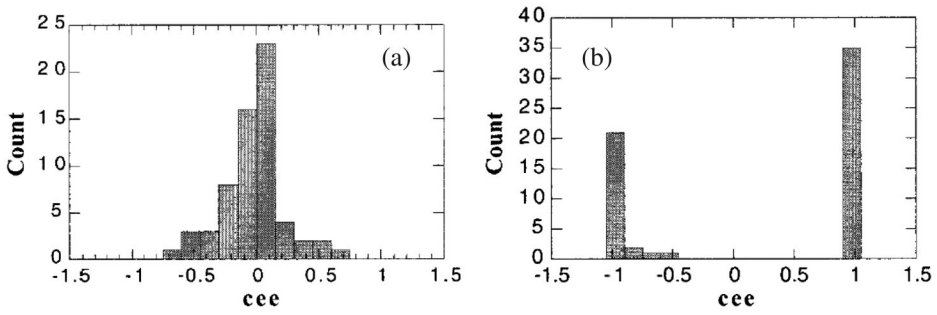

FIG. 5. Distribution of crystalline enantiomeric excess (CEE) for (a) unstirred and (b) stirred crystallizations. From Kondepudi and Asakura, 2001.

dissolved, but excess crystallites of both enantiomorphs remained in the saturated solution. Therefore, the scenario of a single parent crystal could not be valid in this case. Glass beads were added to the solution, and it was strongly stirred with a magnetic stirrer. The glass beads ground the existing crystallites into small pieces. After a few hours, all the crystals existing in the reactor turned out to have the same chirality. The enantiomorph initially in the majority dominated over the minority, and the latter eventually disappeared; thereby the compound attained a homochiral state, as shown in Fig. 3. We analyze this grinding-induced homochirality, called Viedma grinding or Viedma deracemization, in a theoretical Sec. III.C.

B. Experiments with organic crystals

After homochirality was successfully obtained in the growth of the inorganic crystal sodium chlorate (Viedma, 2005), the grinding method was applied to grow homochiral crystals of organic molecules (Noorduin, Izumi *et al.*, 2008; Viedma *et al.*, 2008; Tsogoeva *et al.*, 2009).

Chiral organic molecules can crystallize in two ways. When the cohesion between unlike enantiomer molecules is stronger than that between like enantiomer molecules, different enantiomers are incorporated into a single crystal, and a racemic compound or a racemate is formed. In the opposite case, when the cohesion between like enantiomer molecules is stronger than that between unlike enantiomers, each enantiomer crystallizes into its respective single crystal. A crystal thus formed is called a conglomerate. We consider the latter conglomerate system, where crystallization is chiroselective. After completion of the usual solution growth of conglomerate crystals without grinding, there remain equal amounts of small crystallites of the two enantiomers in the reactor, and as a whole the system is racemic. However, the process of grinding alters this situation, thereby leading to homochirality.

1. Chirality conversion in solution (Noorduin *et al.*)

Noorduin, Izumi *et al.* (2008) succeeded in homochiral crystal growth of a chiral organic molecule, the imine of 2-methyl-benzaldehyde and phenylglycinamide. The constituent molecules are chiral, and they form a conglomerate. A molecule can change its chirality only when it is isolated in the solution as a monomer, provided that the solution contains a particular additive. In contrast, once a molecule is incorporated in a crystal cluster, it can no longer change its chirality.

Using the method of grinding with glass beads, Noorduin *et al.* observed that all the molecules switch their chirality to a single enantiomer; homochirality at the molecular level was achieved. They observed that the EE increases exponentially in time until it reaches unity.

The process was also successfully applied to the crystallization of an amino acid (Viedma *et al.*, 2008).

2. Reaction in solution (Tsogoeva *et al.*)

Tsogoeva *et al.* (2009) crystallized another organic molecule that forms a conglomerate. However, in this case, the monomer in the solution changes its chirality through a reversible chemical reaction via achiral reactants. Even with this complex process of chirality conversion, homochirality was achieved after crystal growth from a stirred solution.

C. Theoretical models

There are many theories to explain homochirality based on rate equations (Uwaha, 2004, 2008; Saito and Hyuga, 2005a; McBride and Tully, 2008). Nonlinearity in these studies is introduced by assuming that small chiral units are formed and are incorporated in crystallites, even when the monomers are chiral (Uwaha, 2008). As another possibility for elucidation of homochirality in crystal growth under grinding, especially in order to identify the origin of nonlinearity, Saito and Hyuga (2008, 2009, 2010, 2011) proposed simple lattice-gas models and studied them using kinetic Monte Carlo (KMC) simulations.

1. *ARS* model

The simplest model is the one in which achiral molecules crystallize into chiral crystal clusters (Saito and Hyuga, 2010). On a square lattice, each site is occupied by an achiral molecule A, or a chiral molecule R or S, or by a solvent molecule. Since the solvent is inactive and acts only as the background, the site occupied by the solvent is denoted as "empty" hereafter. Double occupancy of a site is forbidden. The total concentration of active molecules A, R, and S is fixed at c.

The initial state is chosen achiral such that only A molecules are distributed randomly in the simulation box. These A molecules jump to arbitrary empty sites. The long-ranged jump mimics the process of strong stirring during crystal growth, and diffusional transport plays a negligible role. When two A molecules happen to be positioned at the nearest-neighbor (NN) sites, they can bond and form a dimer which is assumed to acquire chirality to become either R_2 or S_2. The rate of dimer formation k_0 is equal for the two enantiomers. Chiral clusters are assumed to be immobile for simplicity, and they grow in size by converting achiral molecules at their periphery to chiral molecules with the same chirality that they have. For simplicity, temperature is assumed so low that chiral clusters once formed will not dissociate; the crystal growth is irreversible. With this irreversible growth, there is no possibility of Ostwald ripening.

With only irreversible crystal growth, it is clear that crystallization stops when all the achiral molecules become chiral, R or S. Since the growth of R and S crystal clusters is equivalent, a racemic mixture of R and S crystallites is obtained, as shown in Fig. 6(a). The value of the CEE $|\phi|$ remains fairly small.

Grinding greatly changes the situation. It crushes crystal clusters into many small fragments and redistributes them. The fragmentation and redistribution effects are modeled in the following manner in simulations. First the whole system is divided into small square cells, and each cell is further divided by diagonals into four triangles. Then the upper and lower or left and right triangles of each cell are randomly exchanged, and finally all the cells are randomly rearranged in position. Because of this grinding procedure, growing crystals are cut into small fragments, sometimes even to the

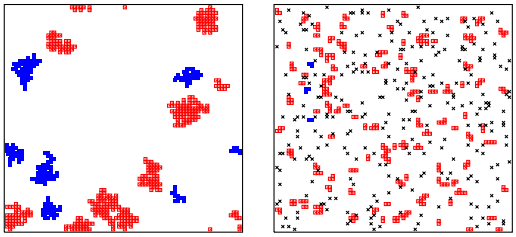

(a) (b)

FIG. 6 (color online). Final configuration of two enantiomers, R (open square) and S (filled square), and an achiral molecule A (cross) in the ARS model. (a) Without and (b) with grinding. From Saito and Hyuga, 2010.

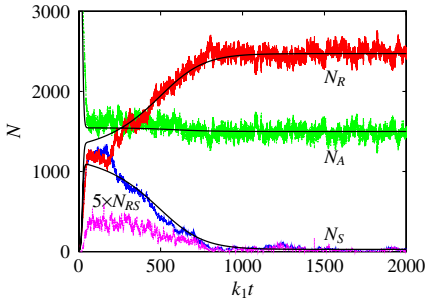

FIG. 7 (color online). Time variation of the population numbers of A, R, and S molecules as well as the number of RS pairs when the crystals are ground. Curves represent fits by the rate equation (3.1). From Saito and Hyuga, 2010.

level of a monomer. Since a monomer has no chirality, it is recycled back into an achiral molecule A.

In KMC simulations with grinding, the time evolution of the population numbers N_A, N_R, and N_S of A, R, and S molecules is divided into three stages, as shown in Fig. 7. In the early stage N_R and N_S increase rapidly at almost identical rates at the expense of N_A. In the intermediate stage, N_R is almost the same as N_S, and they remain constant. In this period, R and S enantiomorphs are in competition. In the last stage, one enantiomorph starts to dominate over the other. The population of the winner increases at the cost of that of the loser. There is no preference for the choice of the winner; it is random.

The final configuration under grinding is shown in Fig. 6(b). There are many small chiral clusters R and S and a finite number of achiral molecules A. The population densities of the two chiral clusters are clearly different; chiral symmetry is broken. However, in Fig. 6(b), a small amount of minority enantiomorph still remains, and the system is not homochiral. This is due to the recycled achiral monomer A, since the random spontaneous dimerization inevitably produces both R and S enantiomorphs. The quantity of the minority enantiomorph decreases as the spontaneous nucleation rate k_0 decreases.

We now examine the mechanism for this chiral symmetry breaking. The characteristic feature in Fig. 6(b) is that the crystal clusters are small and exhibit almost identical size irrespective of the chirality. In addition, due to the recycling effect, there are many achiral monomers A remaining. Another feature apparent in Fig. 7 is that in the intermediate stage when the two enantiomorphs are competing, the number of neighboring RS pairs N_{RS} increases. This means that the R and S crystal clusters often come in contact. Consequently, we suppose the following scenario. A crystal cluster grows by incorporating achiral molecules A at its periphery. Since the size of the clusters is constant on average, the total perimeter of chiral clusters is proportional to the total number of chiral molecules or their concentrations r and s. Therefore, the concentration increase per unit time is linearly proportional to the product of the concentration of r or s and that of the achiral molecule a. The achiral molecule is consumed during crystallization, but it is constantly supplied by grinding; it is recycled from chiral crystals. On the other hand, when the numbers of R and S molecules or clusters increase, the number of RS contacts increases, as shown in Fig. 7. When two clusters of opposite enantiomorphs come in contact, as shown in Fig. 8, the growth points at cluster peripheries are covered, and these points are not available to the achiral molecule A. The growth rates of both enantiomorphs are suppressed, and this corresponds to the mutual antagonism proposed by Frank (1953).

We formulate the above scenario into rate equations. For the growth of R and S crystals with concentrations r and s, we have

$$\begin{aligned} \frac{dr}{dt} &= \tilde{k}_0 a^2 + \tilde{k}_1 ar - \lambda r - \tilde{\mu} ars, \\ \frac{ds}{dt} &= \tilde{k}_0 a^2 + \tilde{k}_1 as - \lambda s - \tilde{\mu} ars. \end{aligned} \tag{3.1}$$

The first term on the right-hand side (rhs) represents the nucleation of a chiral dimer from two neighboring achiral molecules A. The second term corresponds to the peripheral incorporation of achiral molecules into chiral clusters, the third corresponds to grinding-induced recycling of achiral molecules, and the last term corresponds to mutual antagonism due to the proximity of opposite enantiomorphic clusters. The concentration of the achiral molecule a is determined by the conservation of the total concentration $c = a + r + s$, and it varies as $da/dt = -(dr/dt + ds/dt)$. With appropriate choice of the values of the rate constants $\tilde{k}_0$, $\tilde{k}_1$, λ, and $\tilde{\mu}$, the relaxation of the population numbers of the various

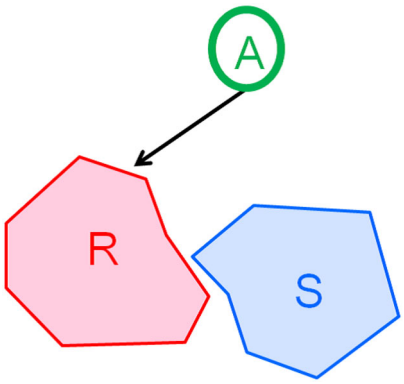

FIG. 8 (color online). Schematic picture of incorporation of achiral molecules on the periphery of a crystal cluster. When two opposite enantiomers are in proximity, the incorporation is mutually suppressed. From Saito and Hyuga, 2011.

molecules obtained in KMC simulation is reproduced, as shown by the smooth curves in Fig. 7.

The development of homochirality is most explicitly observed by transforming the rate equations (3.1) into the time evolution of the chiral order parameter ϕ defined by Eq. (2.5). It is written as

$$\frac{d\phi}{dt} = -\frac{2\tilde{k}_0 a^2}{r+s}\phi + \frac{\tilde{\mu} a(r+s)}{2}\phi(1-\phi^2), \tag{3.2}$$

with $a = c - (r+s)$. The first term represents a decrease in the chiral order parameter due to spontaneous dimerization with the coefficient $\tilde{k}_0$, since it produces both enantiomorphs at random. The process is important in the initial achiral stage when there are no chiral molecules. Once chiral molecules are present, the mutual antagonism introduces a nonlinear effect that is represented by the second term with $\tilde{\mu}$. The nonlinear term resembles that of the Frank model Eq. (2.6), and it leads to chiral symmetry breaking as long as the coefficient $\tilde{\mu} a(r+s)/2$ is positive. However, without recycling, the achiral molecules are consumed such that $a \to 0$ during the growth. Therefore, to maintain a nonvanishing concentration a of the achiral molecules, the recycling process due to grinding is indispensable.

In actual experiments on growth from solution, the crystal growth occurs in diffusion boundary layers around crystal clusters. If the boundary layers of crystallites of opposite enantiomorphs overlap, the crystal growth of both clusters is suppressed, as anticipated in the mutual antagonism scenario. Therefore, mutual antagonism might explain the observed homochirality in the growth from solution of sodium chlorate crystals under grinding.

Cartwright, Piro, and Tuval (2007) simulated crystal growth in a solution confined in a gap between two rotating eccentric cylinders (Metcalfe and Ottino, 1994). Primary nucleation changes achiral monomers into chiral monomers, and they grow in size by incorporating achiral monomers within crystallization range. Because of the shear stress in the chaotic flow, chiral clusters diminish their size by emitting chiral monomers. Chiral monomers lose their chirality and become achiral. (The last process is a recycling process of achiral monomers rather than the Ostwald ripening that Cartwright *et al.* assumed.) The simulation ends up in a homochiral state. We believe that the origin of homochirality in this case is again the mutual antagonism induced by the overlapping of the crystallization zones around different chiral clusters.

2. *RS* model

A similar lattice-gas model has been constructed for the crystal growth of chiral organic molecules (Saito and Hyuga, 2008, 2009). A site on a square lattice is occupied by chiral *R* or *S* molecules, or by a solvent (empty). Chiral monomers randomly jump a long distance to mimic stirring. When two chiral molecules of the same handedness come in contact at NN sites, they can bond and form a conglomerate crystal cluster. It is assumed that no mixed crystals are formed. Crystal cohesion is modeled by assigning a lower jump rate to a molecule with more NN bonds, so that molecules in a crystal cluster will not easily jump out of it. Chirality conversion is allowed only for isolated monomers as in the experiments (Noorduin, Izumi *et al.*, 2008), and the rate is set as ν_0. Simulation starts from an achiral initial state with equal amounts of *R* and *S* monomers.

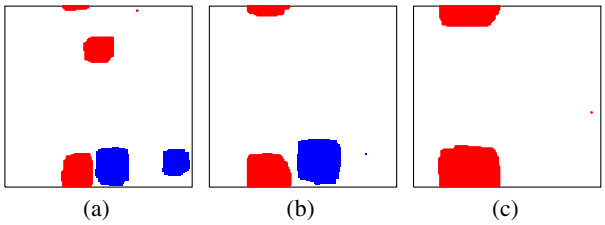

FIG. 9 (color online). Without grinding, homochirality is accomplished by Ostwald ripening after a long time. From Saito and Hyuga, 2009.

Without grinding, several small clusters are nucleated at an early stage [see Fig. 9(a)], and they coarsen by Ostwald ripening (OR) among like enantiomeric crystals; larger clusters dominate over smaller ones due to the curvature effect. Consequently, two large crystal clusters of different enantiomers remain, as shown in Fig. 9(b). Further OR between the two remaining clusters of different enantiomers is very slow since it is limited by dissolution of clusters to emit monomers and by subsequent slow chirality conversion of monomers [see Fig. 9(c)]. A similar slow OR process is actually observed in experiments (Noorduin, Meeks *et al.*, 2008).

With grinding the system is found to settle fairly rapidly to the homochiral state, as shown in Fig. 10(b) (Saito and Hyuga, 2009). In the early racemic stage, there are many small crystal clusters of similar sizes [see Fig. 10(a)]. During chirality competition, until the final homochiral state, the average size of these clusters remains constant, as shown in Fig. 10. Chirality conversion occurs such that the population density of the crystal clusters of one enantiomeric type increases at the cost of that of the opposite type.

We now consider the mechanism of chiral symmetry breaking to homochirality in terms of the relevant rate equations. The role of the achiral molecule *A* in the *ARS* model is now shared by the monomers of the chiral enantiomers *R* and *S*. Therefore, the concentrations of monomers should be treated separately from the concentrations of chiral molecules incorporated in crystal clusters; the former are denoted as r_1 and s_1, and the latter as r_c and s_c. Monomers change their chirality with a rate ν_0. When two monomers of the same chirality come in contact, they form the nucleus of a crystal

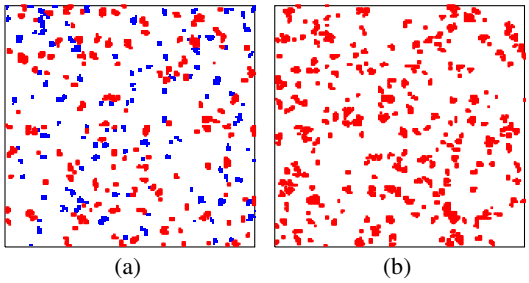

FIG. 10 (color online). Cluster configuration under grinding (a) in the intermediate racemic state, and (b) the final homochiral state. From Saito and Hyuga, 2009.

cluster. Clusters grow by incorporating monomers of the same enantiomeric type at their periphery. Since the sizes of crystal clusters are constant on average, their peripheral length is proportional to the concentrations of the enantiomers in crystal clusters, r_c and s_c. The monomers are recycled by grinding crystal clusters. The process of mutual antagonism introduced in the previous section for the *ARS* model still holds in this *RS* model, since the proximity of the opposite enantiomeric clusters shields the peripheries of both types of crystal cluster. All these processes are summarized in the following rate equations:

$$\begin{aligned}
\frac{dr_1}{dt} &= -\nu_0(r_1 - s_1) - \frac{dr_c}{dt}, \\
\frac{dr_c}{dt} &= \tilde{k}_0 r_1^2 + \tilde{k}_1 r_1 r_c - \lambda r_c - \tilde{\mu} r_1 r_c s_c, \\
\frac{ds_1}{dt} &= \nu_0(r_1 - s_1) - \frac{ds_c}{dt}, \\
\frac{ds_c}{dt} &= \tilde{k}_0 s_1^2 + \tilde{k}_1 s_1 s_c - \lambda s_c - \tilde{\mu} s_1 r_c s_c.
\end{aligned} \tag{3.3}$$

When the racemization rate ν_0 is very large, or at a steady state when there is no time variation of any concentration ($\dot{r}_1 = \dot{r}_c = \dot{s}_1 = \dot{s}_c = 0$), the concentrations of the monomers of the two enantiomers should be equal, i.e., $r_1 = s_1$. Consequently, Eq. (3.3) will have the same final state of spontaneously broken chiral symmetry as that in the case of the *ARS* system; the concentration of the achiral molecule a is replaced by the concentrations of the chiral monomers $r_1 = s_1$, and the concentrations of the chiral molecules r and s are replaced by those in chiral crystals, r_c and s_c. The rate equations (3.3) produce a good fit to the time evolution of the population numbers of the chiral molecules obtained in a KMC simulation if appropriate values of the various rate constants are chosen, as shown in Fig. 11 (Saito and Hyuga, 2011).

The steady state thus obtained under grinding, shown in Fig. 10, consists of many small crystal clusters, and it is unfavorable with respect to the surface free energy. The true equilibrium state should be the state with a single large crystal [as shown in Fig. 9(c)] after Ostwald ripening. The grinding keeps the system away from equilibrium by introducing the energy necessary to break the crystals and create new surfaces.

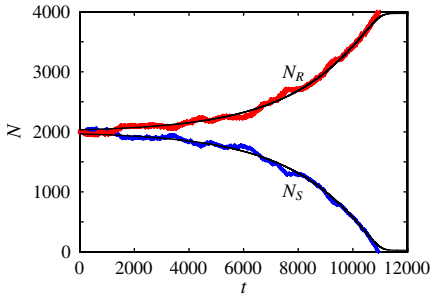

FIG. 11 (color online). Time variation of the population numbers of R and S molecules. Curves represent the fit to the rate equation (3.3). From Saito and Hyuga, 2011.

IV. CHIRALITY SELECTION IN CHEMICAL REACTIONS

It was 40 years before the model proposed by Frank was realized as a practical chemical reaction system. Such a chemical reaction system that involves an autocatalytic process was discovered by Soai *et al.* (1995). In the Soai reaction, the EE was amplified, although the system did not attain homochirality. We first briefly summarize these experimental results and then present theoretical studies on how to achieve homochirality (Saito and Hyuga, 2004) and further analysis on its stochastic aspects (Saito, Sugimori, and Hyuga, 2007).

A. Soai reaction

1. Soai reaction

The Soai reaction is an alkylation of aldehydes in which an aldehyde A reacts with a metallic compound B to produce an alcohol C (Soai *et al.*, 1995). Examples of such substances are 2-alkynylpyrimidine-5-carbaldehyde (A), diisopropylzinc (B), and 2-alkynyl-5-pyrimidyl alkanol (C) (Sato *et al.*, 2001). Although the reactant molecules A and B are achiral, the product molecule C has a chirality; (R)-C and (S)-C, simply called R and S hereafter. The reactants A and B are dissolved in a solvent, and to them is added a small amount of an R and S mixture that has a small imbalance or initial bias in the EE, $|\phi_0|$. When the reaction is complete, the reactant molecules A and B afford product C with high yield, and the final EE value $|\phi_\infty|$ is found to be larger than the initial value $|\phi_0|$. Thus the EE is amplified, although the final EE is not 100%. The initially added products act as an enantioselective catalyst for the production of the same type of enantiomers. In order to amplify the EE value further, Soai *et al.* used a product with higher EE as a new catalyst, and the reaction was iterated several times, as shown in Fig. 2. They were able to obtain an EE value of more than 99% (Sato, Urabe *et al.*, 2003).

Soai *et al.* also proved that chirality selection is very sensitive to the chiral initiators, which are different from the products themselves. They found, for example, that quartz (Soai *et al.*, 1999), $NaClO_3$ (Sato, Kadowaki, and Soai, 2000), and polarized light (Kawasaki *et al.*, 2005) are very good chiral initiators to select one enantiomer over the other with a high EE amplification. Recently, it was shown that even isotopes can trigger EE amplification (Kawasaki *et al.*, 2009). These experiments clearly indicate that homochirality is readily accomplished from a small initial chirality bias if an EE amplification mechanism is provided.

2. Second-order autocatalysis

Since the discovery of EE amplification, the molecular mechanism for the EE amplification has been studied; the homodimer is supposed to act as the catalyst (Blackmond *et al.*, 2001; Sato *et al.*, 2001; Gridnev *et al.*, 2003; Sato, Omiya *et al.*, 2003; Blackmond, 2004). We explain the autocatalytic mechanism by considering the description provided by Sato *et al.* (2001) and Sato, Omiya *et al.* (2003). They assumed the following set of chemical reactions:

$$\text{homo: } R + R \leftrightarrow RR, \qquad S + S \leftrightarrow SS, \tag{4.1a}$$

$$\text{hetero: } R + S \leftrightarrow RS, \tag{4.1b}$$

$$k\text{: } A + B + RR \rightarrow R + RR, \quad A + B + SS \rightarrow S + SS, \tag{4.1c}$$

$$k'\text{: } A + B + RS \rightarrow R + RS, \quad A + B + RS \rightarrow S + RS. \tag{4.1d}$$

Equations (4.1a) and (4.1b) represent the formation of homodimers (RR and SS) and heterodimers (RS), respectively. These reactions are reversible and assumed to occur sufficiently quickly that the dimer concentrations $[RR]$, $[RS]$, and $[SS]$ are quasistationary, i.e., $d[RR]/dt = d[SS]/dt = d[RS]/dt = 0$. Consequently, they are determined by the monomer concentrations r and s as

$$[RR] = Kr^2, \qquad [SS] = Ks^2, \qquad [RS] = K'rs \tag{4.2}$$

with the equilibrium constants K and K'. Under the quasistationary assumption Eq. (4.2), the rate equations for the concentrations r and s of the chiral monomers R and S are derived as

$$\frac{dr}{dt} = kKabr^2 + k'K'abrs, \tag{4.3a}$$

$$\frac{ds}{dt} = kKabs^2 + k'K'abrs. \tag{4.3b}$$

In Eq. (4.3a), which describes the variation of the concentration of the R enantiomer, the first term on the rhs represents the autocatalytic process of a homodimer, and it is of the second order such that two R enantiomers are required in the production of an R enantiomer from achiral reactants A and B. The second term corresponds to the autocatalytic reaction of a heterodimer, and it is of the first order for R and S enantiomers. The conservation of materials requires that the concentrations a and b of achiral reactants A and B should satisfy the relations $a + r + s = \text{const}$ and $b + r + s = \text{const}$.

The time evolution of the yield $r + s$ and of the EE value $|\phi|$ observed in the experiments is well reproduced by fitting the solution of the rate equations (4.3a) and (4.3b) with appropriate values of the reaction rates k and k' as well as the equilibrium constants K and K' (Sato, Omiya *et al.*, 2003). In some cases, the effect of a heterodimer is negligible, i.e., $k'K' = 0$, or it should at least be small compared to the contributions from the homodimers, i.e., $k'K' < kK$ (Blackmond *et al.*, 2001; Sato *et al.*, 2001; Buhse, 2003; Sato, Omiya *et al.*, 2003). Thus autocatalysis via homodimers or that of the second order seems to explain the EE amplification in the experiments. More detailed studies of the molecular mechanism of autocatalysis are currently under way (Blackmond, 2004; Gridnev and Brown, 2004; Islas *et al.*, 2005; Ercolani and Schiaffino, 2011).

3. Soai reaction without chiral initiator

Many researchers have performed the Soai reaction starting from a completely achiral initial state (Singleton and Vo, 2002, 2003; Soai *et al.*, 2003; Gridnev, 2006; Kawasaki *et al.*, 2006). After repetition of the experiment with many samples, it is found that the final EE value varies from sample to sample. Sometimes the R enantiomer is the majority, and sometimes the S enantiomer is. The value of the order parameter ϕ can be positive or negative. Its distribution has two peaks at almost symmetric points, as shown in Fig. 12 (Soai *et al.*, 2003).

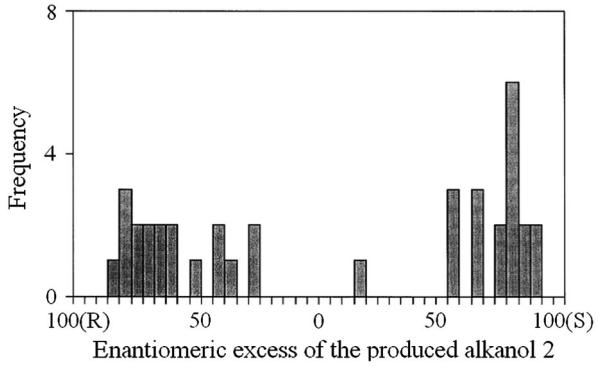

FIG. 12. Frequency of the enantiomeric excess of the alkanol produced without initial chiral ingredients. Adapted from Soai *et al.*, 2003.

To study the corresponding probability distribution, as presented in experiments (Soai *et al.*, 2003; Kawasaki *et al.*, 2006), the rate equation approach is not valid, and a stochastic analysis is necessary. The analysis was initiated by Lente (2004) up to first-order autocatalytic processes, and it was extended to second order by Saito, Sugimori, and Hyuga (2007).

B. Theoretical analyses

To understand the essential features of EE amplification observed in the Soai reaction and to search for possible ways to attain homochirality, Saito and Hyuga (2004) studied a simple chemical reaction model. In this model, it is assumed that there is an ample amount of achiral reactant B so that its time variation is discarded, and only the achiral molecule A is considered. Consequently, the conservation of the total material imposes the condition

$$a + r + s = c = \text{const}. \tag{4.4}$$

With the restriction that the concentration variables r, s, and $a = c - r - s$ are all non-negative, the r-s phase space is limited to the triangular region defined by $0 \le r$, s, and $r + s \le c$.

Chiral enantiomers are irreversibly produced (a) spontaneously, (b) by a linear (or first-order) autocatalytic process, and (c) by a nonlinear (or second-order) autocatalysis. It will be shown later that these processes are sufficient to explain EE amplification, but for the establishment of homochirality (d) the recycling process which converts chiral products R and S enantiomers to an achiral reactant A is necessary. All together, the relevant reaction schemes are described as

$$k_0\text{: } A \rightarrow R, \qquad A \rightarrow S, \tag{4.5a}$$

$$k_1\text{: } A + R \rightarrow 2R, \qquad A + S \rightarrow 2S, \tag{4.5b}$$

$$k_2\text{: } A + 2R \rightarrow 3R, \qquad A + 2S \rightarrow 3S, \tag{4.5c}$$

$$\lambda\text{: } R \rightarrow A, \qquad S \rightarrow A, \tag{4.5d}$$

with respective rate constants k_0, k_1, k_2, and λ.

The rate equations for the concentrations r and s of the R and S enantiomers, respectively, are written as

$$\frac{dr}{dt} = (k_0 + k_1 r + k_2 r^2)a - \lambda r, \tag{4.6a}$$

$$\frac{ds}{dt} = (k_0 + k_1 s + k_2 s^2)a - \lambda s. \tag{4.6b}$$

From Eqs. (4.6a) and (4.6b), we derive the time evolution of the chiral order parameter $\phi = (r - s)/(r + s)$ as follows:

$$\frac{d\phi}{dt} = -k_0 \frac{a}{r+s}\phi + k_2 \frac{a(r+s)}{2}\phi(1 - \phi^2). \tag{4.7}$$

This equation appears similar to that of the Frank model, Eq. (2.6), and crystal growth, Eq. (3.2). The coefficients of neither the linear autocatalysis, k_1, nor the recycling process, λ, appear explicitly in Eq. (4.7). They are hidden in the time dependence of the achiral concentration $a(t)$ and the symmetric combination $r(t) + s(t)$ $[= c - a(t)]$. Since a and $r + s$ are non-negative, the spontaneous production, denoted by k_0, leads to decay of the chiral order parameter ϕ. Only nonlinear autocatalysis, denoted by k_2, can provide the amplification of ϕ. However, for homochirality to be achieved, the coefficient of the nonlinear term $k_2 a(r + s)/2$ should remain positive at all times.

Comparison of Eqs. (4.6a) and (4.6b) with Eqs. (4.3a) and (4.3b) shows that k_2 corresponds to kKb of the homodimer autocatalysis. When the heterodimer also acts as a catalyst, the coefficient of the nonlinear term in Eq. (4.7) is modified to $(kK - k'K')ab(r + s)/2$, thereby indicating the racemization effect of the heterodimer. The heterodimer's racemization effect should be smaller than the deracemaization effect of the homodimer, $k'K' < kK$, for EE amplification or homochirality.

1. Without recycling: EE amplification

Equation (4.7) ensures the amplification of the chiral order parameter as long as the coefficient $k_2 a(r + s)/2$ is positive. However, the Soai reaction is performed in a closed reactor without recycling ($\lambda = 0$), and the reaction proceeds irreversibly in the forward direction. Eventually, the achiral reactant is exhausted ($a = 0$), and the reaction stops. The state with $a = 0$ or $r + s = c$ corresponds to a line of fixed points ($dr/dt = ds/dt = 0$) of the rate equations (4.6a) and (4.6b), if $\lambda = 0$. When the reaction stops, so does the EE amplification. Therefore, EE amplification occurs, but a homochiral state cannot be achieved without recycling.

For a few simple cases, the trajectory of the reaction flow in the r-s phase space can be easily calculated by integrating dr/ds obtained from Eqs. (4.6a) and (4.6b).

a. Spontaneous production ($k_0 > 0$, $k_1 = k_2 = \lambda = 0$)

The flow trajectory in r-s phase space is a line $r = s + r_0 - s_0$ that terminates at the fixed line $r + s = c$. Here r_0 and s_0 are initial concentrations. The EE value $|\phi|$ decreases in time, since the numerator $(r - s)$ in the definition (2.5) of ϕ remains constant, while the denominator $(r + s)$ increases as the reaction proceeds.

b. Linear autocatalysis ($k_1 > 0$, $k_0 = k_2 = \lambda = 0$)

The trajectory $r = (r_0/s_0)s$ is a line radiating from the origin. Since the ratio r/s does not change in time, the chiral order parameter remains constant. Linear autocatalysis promotes the production of the same enantiomeric type, but the majority-to-minority ratio does not change. Enantiomeric excess amplification is not possible with only linear autocatalysis.

c. Nonlinear autocatalysis ($k_2 > 0$, $k_0 = k_1 = \lambda = 0$)

With only nonlinear autocatalysis k_2, the flow trajectory is a hyperbola passing through the origin, $1/r - 1/s = 1/r_0 - 1/s_0$, and terminates on the fixed line, as shown in Fig. 13(a). If $r_0 > s_0$, the trajectory bends toward larger r values, and the chiral order parameter ϕ increases with EE amplification. This is evident from the relation of the final value of the EE order parameter $|\phi_\infty|$ versus its initial value $|\phi_0|$, shown in Fig. 14.

2. With recycling: Homochirality

Without recycling the EE amplification stops at an intermediate level because the achiral reactant is completely consumed ($a_\infty = 0$). If one could supply an achiral reactant, then EE amplification would continue and homochirality would be achieved. Supply is possible by recycling the achiral reactant A from the chiral products R and S. This is the process with a coefficient λ in Eqs. (4.6a) and (4.6b), even though it does not explicitly affect the time evolution of ϕ, as indicated by Eq. (4.7).

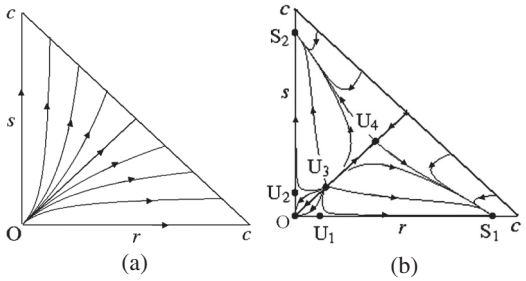

FIG. 13. Flow diagrams in the r-s phase space with nonlinear autocatalysis (a) without and (b) with recycling. From Saito and Hyuga, 2004.

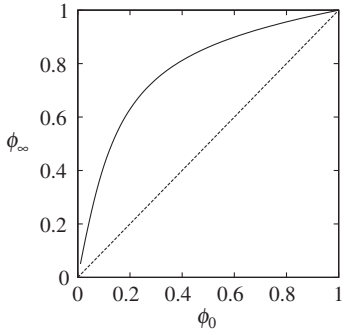

FIG. 14. Final value of the chiral order parameter ϕ_∞ vs initial value ϕ_0 with nonlinear autocatalysis but without recycling. Initially, achiral molecules comprise 80% of all reactive substances.

The recycling process drastically alters the flow trajectory in the r-s phase space. The line $r + s = c$ is no longer a line of fixed points, but the system has several fixed points.

a. Spontaneous production ($\lambda > 0,\ k_0 > 0,\ k_1 = k_2 = 0$)

There is only a racemic fixed point at $r^* = s^* = k_0 c/(2k_0 + \lambda)$. This is consistent with the evolution equation (4.7), which indicates that ϕ should reduce to zero.

b. Linear autocatalysis ($\lambda > 0,\ k_1 > 0,\ k_0 = k_2 = 0$)

The system has a trivial and unstable fixed point $r = s = 0$, and a fixed line which is shifted to $a = \lambda/k_1$. This fixed line is structurally unstable such that with small spontaneous production k_0, the fixed line collapses to a racemic fixed point.

c. Nonlinear autocatalysis ($\lambda > 0,\ k_2 > 0,\ k_0 = k_1 = 0$)

If the recycling coefficient λ is small enough ($\lambda < k_2 c^2/8$), the system has seven fixed points, as shown in Fig. 13(b). Four of them are unstable, and three are stable. One stable fixed point is a trivial one $(r, s) = (0, 0)$. The other two stable fixed points are homochiral at $(r, s) = (X, 0)$ or $(0, X)$ with $X = (c + \sqrt{c^2 - 4\lambda/k_2})/2$. Thus, homochirality is achieved by introducing the recycling process, as already anticipated from Eq. (4.7).

3. Origin of recycling

What is the origin of the recycling process and how can it be introduced in a reaction system? The reverse chemical reaction is found to be inappropriate as a candidate for the recycling process, since it always leads to an equilibrium state which is racemic (Saito and Hyuga, 2005b; Blackmond and Matar, 2008). Therefore, the system has to be driven out of equilibrium (Saito and Hyuga, 2005b; Plasson, 2008).

a. Reverse reactions

Since the recycling process from the chiral products R or S to the achiral reactant A corresponds to the reverse of the spontaneous production from A to R or S, the reverse chemical reaction is a natural candidate for the recycling process. However, one has to be careful about the microscopic processes involved in chemical reactions (Blackmond and Matar, 2008). In the reaction coordinate that represents the variation of chemical potential as a function of molecular states, as shown in Fig. 15(a), the chemical reaction proceeds such that a reactant A with a high chemical potential μ_A passes through a transition state with a higher chemical potential to the product R or S with the lower chemical potential $\mu_R = \mu_S$. The forward reaction rate k_0 through path (i) in Fig. 15(a) is controlled by the thermal activation process needed to cross the intermediate energy barrier. The rate of the reverse reaction $k_0^{(-)}$ is smaller than the forward rate k_0, because of an additional energy barrier due to the chemical potential difference $\Delta\mu = \mu_A - \mu_R$; the reverse reaction rate is $k_0^{(-)} = k_0 e^{-\Delta\mu/k_B T}$. With $k_0^{(-)}$ the states with broken chiral symmetry ($r \neq s$) remain stable, as long as k_0 is very small compared to the rate of the autocatalytic process $k_2 c^2$.

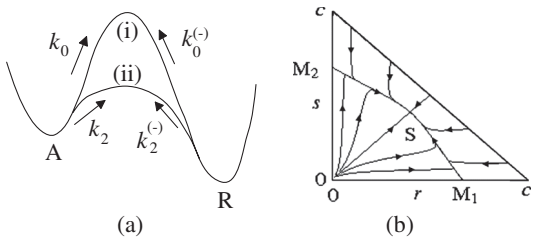

FIG. 15. System with reverse reactions. (a) Reaction paths in a free energy landscape in a reaction coordinate. (i) Spontaneous production of R from A with a rate constant k_0 and its reverse with a rate $k_0^{(-)}$. (ii) Second-order autocatalysis $A + 2R \rightarrow 3R$ with a rate constant k_2 and its reverse with a rate $k_2^{(-)}$. (b) Flow diagram with nonlinear autocatalysis and its reverse reactions (ii).

However, a catalyst is considered to enhance the chemical reaction by lowering the energy barrier at the intermediate transition state, as schematically presented by path (ii) in Fig. 15(a). Consequently, the homodimer catalyst enhances not only the forward reaction, Eq. (4.5c), but also its reverse reaction

$$k_2^{(-)}\colon\ 3R \rightarrow A + 2R, \tag{4.8}$$

where the rate constants are related as (Saito and Hyuga, 2005b; Blackmond and Matar, 2008)

$$\frac{k_2^{(-)}}{k_2} = e^{-\Delta\mu/k_B T} = \frac{k_0^{(-)}}{k_0}. \tag{4.9}$$

If the nonlinear autocatalysis k_2 dominates the spontaneous production k_0, then the dominant reverse process should be associated with $k_2^{(-)}$ rather than $k_0^{(-)}$. If we consider only the two processes with rates k_2 and $k_2^{(-)}$, then the rate equations are

$$\frac{dr}{dt} = k_2 r^2 a - k_2^{(-)} r^3, \qquad \frac{ds}{dt} = k_2 s^2 a - k_2^{(-)} s^3. \tag{4.10}$$

It is noteworthy that $a = c - r - s$. Besides the trivial fixed point $(r, s) = (0, 0)$, there are homochiral fixed points M_1: $(X_h, 0)$ and M_2: $(0, X_h)$ with $X_h = k_2 c/(k_2 + k_2^{(-)})$, and a racemic fixed point S: (X_r, X_r) with $X_r = k_2 c/(2k_2 + k_2^{(-)})$, as depicted in the flow diagram in Fig. 15(b). It is easy to show that the trivial and homochiral fixed points are unstable, and only the racemic fixed point S is stable. Thus, with the reverse reaction $k_2^{(-)}$, the system relaxes to the final equilibrium state, which is racemic. Chiral symmetry cannot be broken in equilibrium. The time evolution of the chiral order parameter is now described as

$$\frac{d\phi}{dt} = \frac{(r+s)\phi}{2}[k_2 a(1-\phi^2) - k_2^{(-)}(r+s)(1+\phi^2)], \tag{4.11}$$

thereby indicating that the reverse reaction $k_2^{(-)}$ always reduces the amplitude of ϕ.

b. Flow in an open system

Since the reverse chemical process is not appropriate for recycling, a physical process under an open system has been

considered (Saito and Hyuga, 2005b). Imagine that the achiral reactant flows into the chemical reactor such that its concentration increases by a quantity F per unit time, as shown in Fig. 16. Simultaneously, the solution with the reactant and products flows out at a constant rate λ such that λa, λr, and λs molecules leave the reactor (see Fig. 16). In the reactor, only the forward reactions equations (4.5a)–(4.5c) occur irreversibly. When the variation in the concentration a of the achiral reactant is included, the rate equations are

$$\frac{dr}{dt} = k(r)a - \lambda r, \qquad \frac{ds}{dt} = k(s)a - \lambda s,$$
$$\frac{da}{dt} = -[k(s) + k(r)]a + F - \lambda a, \tag{4.12}$$

where the autocatalytic rate coefficient is denoted as $k(x) = k_0 + k_1 x + k_2 x^2$ with $x = r$ or s. The first terms on the rhs of the rate equations (4.12) represent chemical reactions, and the remaining terms represent flow contributions. Upon adding the three equations, the total concentration $c = a + r + s$ varies as $dc/dt = F - \lambda c$. In a steady state, the total concentration remains constant, i.e., $c = F/\lambda$. Thus a reaction system with recycling is effectively constructed by bringing the system to a steady state under an open flow.

This constant flow to achieve a homochiral state is similar to the iterative enhancement of EE found in the actual Soai experiments (Sato, Urabe *et al.*, 2003). In the first run, Sato *et al.* added a small amount of an enantiomeric mixture with low EE to achiral reactants, and obtained an EE-amplified final mixture. Subsequently, by using a small amount of the final mixture as an additive to the next achiral reactants, they obtained further enhancement of the EE. The proposed flow scheme appears to be the continuum version of this discrete iteration process. Instead of refilling the reactants after completion of each production process, the flow continuously supplies reactants and removes the product, and the EE is amplified to the limit of unity.

Under the flow, the system is no longer closed but is open. A reactant A with a high chemical potential is supplied externally, and the products R and S with low chemical potentials are drained out of the reactor apparatus. In order to maintain the system in a symmetry-broken state, the system requires the introduction of external energy in the form of a flow.

The possibility of recycling by chemical means was proposed by Plasson (2008). To supply the energy difference associated with the recycling process from the low-energy products R and S to the high-energy reactant A, R and S are supposed to react with a fuel molecule X with a high chemical potential as

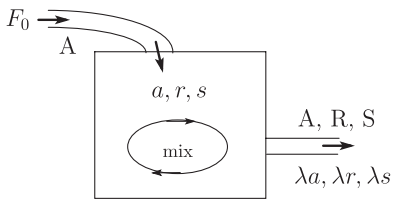

FIG. 16. Reaction system with an open flow.

$$R + X \rightarrow A + Y, \qquad S + X \rightarrow A + Y. \tag{4.13}$$

Here the waste molecule Y has a low chemical potential. Recycling by physical or chemical means requires a supply of external energy to the system.

4. Stochastic analysis of the Soai reaction without chiral initiator

With nonlinear autocatalysis k_2, the chiral order parameter ϕ increases according to Eq. (4.7), as long as the initial bias ϕ_0 is finite. However, if the initial state is achiral with $\phi_0 = 0$, the rate equations (4.6a) and (4.6b) are inadequate since the order parameter ϕ remains zero. On the other hand, experiments show that the final EE value fluctuates for each experimental trial (Singleton and Vo, 2003; Soai *et al.*, 2003; Gridnev, 2006; Kawasaki *et al.*, 2006). The system should be described by a probability distribution (Soai *et al.*, 2003; Kawasaki *et al.*, 2006). Therefore, a theoretical analysis based on a stochastic approach is necessary (Lente, 2004, 2005; Saito, Sugimori, and Hyuga, 2007).

For the stochastic analysis, we abandon the macroscopic description of the system in terms of concentrations. Instead, we use a microscopic description in terms of population numbers N_A, N_R, and N_S of the molecules A, R, and S, respectively, in a reactor of volume V. The total numbers of molecules $N = N_A + N_R + N_S$ is kept constant during chemical reactions. The probability that the system is found in a state $\boldsymbol{X} = (N_A, N_R, N_S)$ at a time t is denoted as $P(\boldsymbol{X}, t)$. A chemical reaction causes a state change from $\boldsymbol{X}$ to $\boldsymbol{X} + \boldsymbol{q}$ with the transition probability $W(\boldsymbol{X}; \boldsymbol{q})$. Here $\boldsymbol{q} = (q_A, q_R, q_S)$ denotes the change of state. For example, when a chiral enantiomer R is produced from an achiral reactant A, the state change is $\boldsymbol{q} = (-1, +1, 0)$, and the transition probability for R production is

$$W(N_A, N_R, N_S; -1, +1, 0) = \kappa(N_R)N_A, \tag{4.14}$$

with

$$\kappa(N_R) = k_0 + \kappa_1 N_R + \kappa_2 N_R^2. \tag{4.15}$$

Here $\kappa_1 = k_1/V$ and $\kappa_2 = k_2/V^2$ are stochastic rate coefficients. The spontaneous production process with rate k_0 is necessary to produce chiral molecules from a completely achiral initial condition without any chiral products; i.e., $N_R = N_S = 0$ at $t = 0$. The recycling from R to A is described by $\boldsymbol{q} = (+1, -1, 0)$ with the transition probability

$$W(N_A, N_R, N_S; +1, -1, 0) = \lambda N_R. \tag{4.16}$$

For the other enantiomer S, there are corresponding production and recycling transition probabilities. The probability $P(\boldsymbol{X}, t)$ varies according to the master equation

$$\frac{dP(\boldsymbol{x}, t)}{dt} = \sum_{\boldsymbol{q}}[W(\boldsymbol{X} - \boldsymbol{q}; \boldsymbol{q})P(\boldsymbol{X} - \boldsymbol{q}, t) - W(\boldsymbol{X}; \boldsymbol{q})P(\boldsymbol{X}, t)]. \tag{4.17}$$

The initial state is set to be achiral with only achiral A molecules and the probability distribution is $P_i = P(\boldsymbol{X}, t = 0) = \delta(N_A - N)\delta(N_R)\delta(N_S)$, where $\delta(x) = 1$ for $x = 0$ and zero otherwise. Then chirality selection is determined by the final probability P_f. If there is a recycling process ($\lambda > 0$), the previous rate equation analysis suggests

a unique final state. Thus, by assuming a detailed balance condition such that the two terms in the square brackets on the rhs of Eq. (4.17) are equal, the final probability distribution is determined as

$$P_f(N_A, N_R, N_S) = \mathcal{N}\frac{N!}{N_A!N_R!N_S!}\lambda^{N_A} f(k_0, \kappa_1, \kappa_2; N_R) \times f(k_0, \kappa_1, \kappa_2; N_S) \tag{4.18}$$

with

$$f(k_0, \kappa_1, \kappa_2; M) = \begin{cases} 1 & \text{for } M = 0, \\ \prod_{m=0}^{M-1} \kappa(m) & \text{for } M \geq 1, \end{cases} \tag{4.19}$$

and a normalization constant $\mathcal{N}$.

With only spontaneous production k_0, P_f has a simple form, given by counting the number of combinations, as $P_f = (N!/N_A!N_R!N_S!)\lambda^{N_A}k_0^{N_R+N_S}/(\lambda + 2k_0)^N$, which has only a racemic peak at $N_R^* = N_S^* = k_0N/(2k_0 + \lambda)$, as shown in Fig. 17(a). The peak position corresponds to the fixed point of the rate equation (see Sec. IV.B.2.a). In the limit of no recycling, $\lambda \to 0$, the final probability is a binomial distribution $P_f = 2^{-N}N!/N_R!(N - N_R)!$ on the fixed line $N_A = 0$ or $N_R + N_S = N$.

By adding a linear autocatalytic process, the final probability distribution broadens sideways, as shown in Fig. 17(b), but there is only a racemic central peak. In the limit of no recycling, $\lambda \to 0$, the probability is finite only on the fixed line $N_A = 0$, and its form reduces to

$$P_f(0, N_R, N - N_R) = \frac{N!}{N_R!(N - N_R)!}\frac{f(k_0, \kappa_1, 0 : N_R)f(k_0, \kappa_1, 0 : N - N_R)}{f(2k_0, \kappa_1, 0 : N)}. \tag{4.20}$$

This final probability (4.20) agrees with the one previously obtained by Lente (2004). The specific feature of this final probability is that it becomes completely flat as $P_f = 1/(N + 1)$ when $\kappa_1 = k_0$. Further, for $\kappa_1 \gg k_0$, P_f has sharp peaks at the two homochiral points $(N_R, N_S) = (N, 0)$ and $(0, N)$. This reflects the fact that by starting from a completely achiral state $N_A = N$ with $N_R = N_S = 0$, there is a lengthy interval of time $\sim(k_0N)^{-1}$ until the first enantiomer is produced spontaneously. The subsequent rapid autocatalytic process κ_1 converts all the achiral reactant molecules A to the first-produced enantiomer type before the second spontaneous production occurs. The situation corresponds to the single-parent scenario.

When nonlinear autocatalysis occurs in addition to spontaneous production, the final probability has double peaks, as shown in Fig. 17(c). The double-peak structure is an indication of phase transition to the chiral state. Indeed, starting from a slightly chiral initial condition, the probability distribution ultimately has a single peak which is off centered, as shown in Fig. 17(d). The other peak observed in Fig. 17(c) is absent.

However, in the absence of recycling, i.e., $\lambda = 0$, the final probability P_f calculated by numerically integrating the master equation (4.17) in time differs from the one obtained from Eq. (4.18) in the limit of no recycling, $\lambda \to 0$. Actually, if the recycling process is absent, the detailed balance condition is no longer valid, and the form (4.18) is not necessarily correct. Therefore, another analysis is necessary, using a directed random walk model. Without recycling, the system consumes only an achiral reactant, and the numbers N_R or N_S of R or S enantiomers increase. Upon plotting the state change in the N_R-N_S phase space, as shown in Fig. 18, the state at (N_R, N_S) jumps to the right by the production of an R enantiomer or up by the production of an S enantiomer. Thus, the chemical reaction is mapped to the directed random walk where a

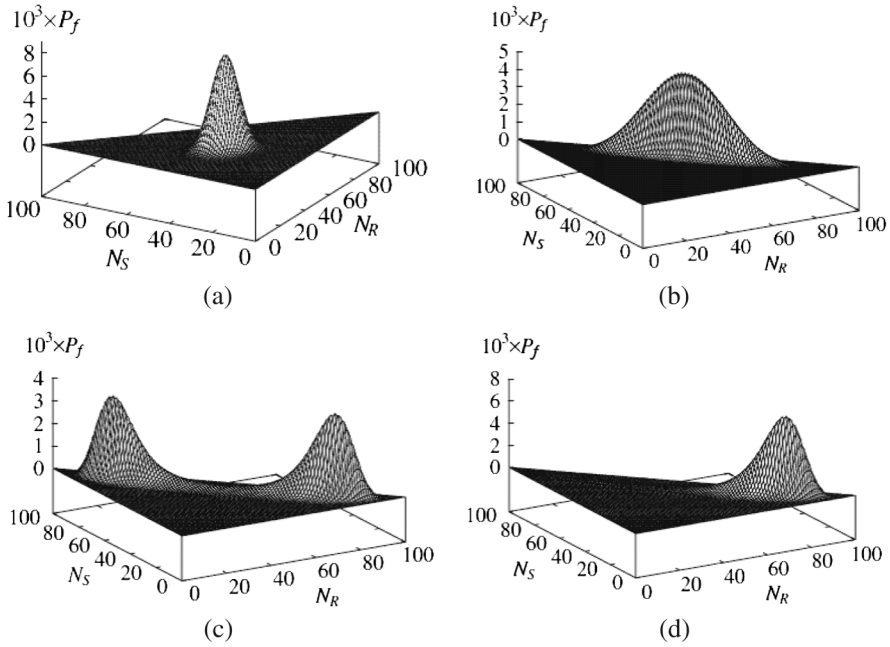

FIG. 17. Probability distribution with recycling. (a) Spontaneous reaction, (b) linear autocatalysis, (c) nonlinear autocatalysis, and (d) with a slightly chiral initial state. From Saito, Sugimori, and Hyuga, 2007.

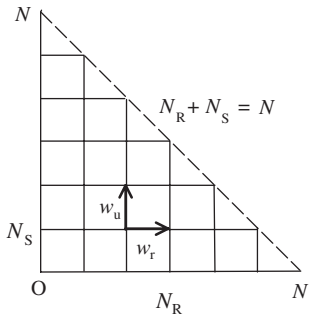

FIG. 18. Directed random walk on a square lattice in N_R-N_S space.

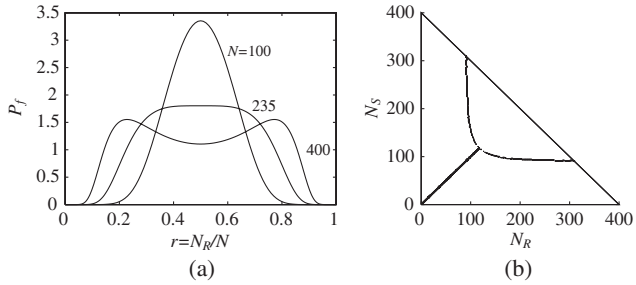

FIG. 19. Final probability distribution P_f for a system with second-order autocatalysis without recycling and without initial chiral ingredients. (a) Profile of P_f depends on the total number of reacting molecules N. If N is small, the system is racemic with only a central peak due to the spontaneous random production of chiral products. If N is large, the autocatalysis eventually dominates over spontaneous formation, and the probability distribution has double peaks. (b) Traces of maximum positions in P_f as the total number N changes. From Saito, Sugimori, and Hyuga, 2007.

walker moves randomly on a square lattice in the N_R-N_S phase space. Since the total number of molecules is fixed as $N = N_A + N_R + N_S$, the phase space is limited to a triangular region (see Fig. 18).

The random walker located at a lattice site (N_R, N_S) waits for a time

$$\tau(N_R, N_S) = \frac{1}{N_A[\kappa(N_R) + \kappa(N_S)]} \tag{4.21}$$

before it jumps. Then it jumps to the right with a probability of $w_r(N_R, N_S) = \kappa(N_R)/[\kappa(N_R) + \kappa(N_S)]$ and up with a probability of $w_u(N_R, N_S) = \kappa(N_S)/[\kappa(N_R) + \kappa(N_S)]$, as indicated in Fig. 18. The transition probability to increase the R enantiomer per unit time is $W(N_r, N_S; +1, 0) = \tau(N_R, N_S)^{-1} w_r(N_R, N_S)$, in agreement with Eq. (4.14). For spontaneous or linear autocatalytic production, the denominator of the waiting time τ depends only on the total number of enantiomeric products as $\kappa(N_R) + \kappa(N_S) = 2k_0 + \kappa_1(N_R + N_S)$. Thus, many random walkers which started at the origin $N_R = N_S = 0$ arrive on the diagonal line $N_R + N_S = N$ at the same time $t = \sum_{n=0}^{N-1}[(N-n)(2k_0 + \kappa_1 n)]^{-1}$. The distribution P_f on this line is simply calculated by counting the possible ways to reach the state (N_R, N_S) from the origin, and it agrees with Eq. (4.20).

With nonlinear autocatalysis, the time when the random walker reaches the diagonal $N_R + N_S = N$ depends on N_R and N_S. However, by disregarding the time development, we can still obtain the final distribution $P_f(N_R, N_S)$ by knowing the P_f's of the neighboring sites before the jump occurred. These can be determined from the master equation,

$$P_f(N_R, N_S) = w_r(N_R - 1, N_S) P_f(N_R - 1, N_S) + w_u(N_R, N_S - 1) P_f(N_R, N_S - 1). \tag{4.22}$$

This relation is valid because only forward jumps occur. The calculated final probability P_f agrees with the one obtained by numerically integrating the original master equation (4.17) (Saito, Sugimori, and Hyuga, 2007). A characteristic feature of P_f in the case of nonlinear autocatalysis is that the profile depends on the total number of reacting molecules N as shown in Fig. 19(a). For a small N value, P_f has only a racemic central peak, whereas for a large N, it has off-centered double peaks at symmetric points. The existence of symmetric double peaks agrees with the experimental findings (Soai *et al.*, 2003; Kawasaki *et al.*, 2006).

As the total number of molecules N increases, the peak position varies in the N_R-N_S phase space, as shown in Fig. 19(b). For a small value of N, there is a single peak on the racemic line $N_R = N_S$. At the critical number N_c, the peak splits into two, and thereafter the two resulting peaks are nearly parallel to the two axes. The trace of the probability maxima in Fig. 19(b) indicates that the population of the majority enantiomer increases, whereas that of the minority remains almost constant, i.e., the production of the minority species is almost stopped. This means that the EE value increases to homochirality, i.e., $|\phi| \to 1$ as N increases. The critical number N_c is found to depend on the ratio of the reaction rates κ_2/k_0. For a small κ_2, a large critical value N_c is required. From numerical studies, N_c is found to be proportional to $(\kappa_2/k_0)^{-3/4}$. The result is analytically elucidated as a crossover in dominant production processes from the spontaneous to the nonlinear autocatalytic process (Saito, Sugimori, and Hyuga, 2007).

V. MODELS FOR HOMOCHIRALITY IN LIFE

In thermal equilibrium, amino acids are known to undergo racemization so that enantiomeric monomers change their chirality over a long period, and the system relaxes to the racemic equilibrium state (Bada, 1985). To sustain homochirality in life or in biomolecules, some external drive is necessary. However, in contrast to the crystal growth or Soai reaction experiments, we have not yet an appropriate experiment that realizes a homochiral state of amino acids or sugars (or nucleotides). Therefore, we restrict our description here to recent progress in various theoretical models. These models are classified into two types depending on whether the autocatalytic process is explicitly required or not.

A. Polymerization model

Amino acids undergo polymerization to form proteins. Nucleotides that contain sugars also polymerize to form DNA and RNA chains. DNA and protein are vital for the present activity of life. After the discovery of the enzymatic

activities of RNA (Kruger *et al.*, 1982; Guerrier-Takada *et al.*, 1983), the RNA world hypothesis was proposed for the origin of life (Gilbert, 1986; Orgel, 2004), because some RNA may carry information and catalytic functions in a single chain. There are other candidates for prebiotic polymers which are simpler than RNA (Orgel, 2004), such as peptide nucleic acid (PNA) (Nelson, Levy, and Miller, 2000) or threose nucleic acid (TNA) (Schoning *et al.*, 2000).

Consequently, various polymerization scenarios for the origin of homochirality have been proposed (Sandars, 2003; Brandenburg *et al.*, 2005; Nilsson *et al.*, 2005; Saito and Hyuga, 2005b), even though PNA is achiral. In oligomerization experiments involving a chiral polymer, it is found that a monomer of the same chirality as the chain can be incorporated readily to extend the chain, whereas that of opposite chirality is found to terminate the chain (Joyce *et al.*, 1984; Feringa and van Delden, 1999). Therefore, polymerization models include the effect of cross inhibition such that when an unlike enantiomer polymerizes at one end of the chain, the polymerization at this end is terminated. The process is thought to correspond to the idea of mutual antagonism in the Frank model. Another feature that is taken into account in polymerization models is autocatalysis, since proteins and some RNA molecules act as enzymes to catalyze chemical reactions. Therefore, theories assume that a long homopolymer acts as a catalyst for the production of an enantiomeric monomer of the same type. With these two features, the model appears analogous to Frank's model, and numerical calculations show chiral symmetry breaking (Sandars, 2003).

B. APED model

The problem with the polymerization model is that the catalytic effect normally appears only for very long and complex polymers. Therefore, a model that does not explicitly require autocatalysis has been proposed by Plasson, Bersini, and Commeyras (2004). Instead of autocatalysis, the model incorporates the fact that a monomer in a heterodimer can change its chirality due to its opposite partner. This process is called epimerization, and it is known to occur with amino acids in peptides or proteins (Kriausakul and Mitterer, 1978).

The original model (Plasson, Bersini, and Commeyras, 2004) consists of 11 elementary processes, but later studies show that the five processes shown in Fig. 20 are essential

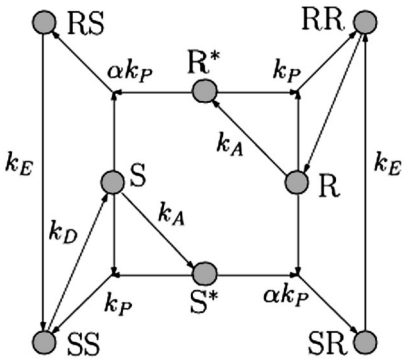

FIG. 20. Simplified APED model. Adapted from Brandenburg, Lehto, and Lehto, 2007.

(Brandenburg, Lehto, and Lehto, 2007). We explain the model in the latter simplified version by first presenting the reaction schemes, followed by the explanations of each process. In the original paper, D/L representation is used since Plasson, Bersini, and Commeyras were referring to amino acids. However, here we use the R/S representation to unify the notation:

The reaction processes are

$$k_A\colon R \rightarrow R^*, \qquad S \rightarrow S^*, \tag{5.1a}$$

$$k_P\colon R^* + R \rightarrow RR, \qquad S^* + S \rightarrow SS, \tag{5.1b}$$

$$\alpha k_P\colon R^* + S \rightarrow RS, \qquad S^* + R \rightarrow SR, \tag{5.1c}$$

$$k_E\colon RS \rightarrow SS, \qquad SR \rightarrow RR, \tag{5.1d}$$

$$k_D\colon RR \rightarrow R + R, \qquad SS \rightarrow S + S. \tag{5.1e}$$

Activation (5.1a): Polymerization is possible only when the enantiomeric monomers are activated externally.

Polymerization (5.1b) and (5.1c): The activated monomer polymerizes to the unactivated enantiomer from one side. This reflects the fact that the two termini of polymers are inequivalent; the heterodimers RS and SR are different. For simplicity, the polymerization level is limited to dimers in the model. Heterodimers in Eq. (5.1c) are assumed to be produced less efficiently than homodimers in Eq. (5.1b). Therefore, the parameter α lies between 0 and 1.

Epimerization (5.1d): In heterodimers epimerization occurs only with the enantiomer at the left terminus. Because of this epimerization, heterodimers will change to homodimers after a while.

Depolymerization (5.1e): Homodimers decompose to unactivated monomers. The depolymerization process recycles the monomers, and this process is necessary to achieve homochirality. Otherwise, the system stops evolution when whole monomers are dimerized. Since the model consists of essentially four processes (activation, polymerization, epimerization, and depolymerization), it is called the APED model.

The rate equations for the various concentrations are written as

$$\begin{aligned} dr/dt &= -k_A r - k_P r r^* - \alpha k_P r s^* + 2k_D[RR], \\ dr^*/dt &= k_A r - k_P r r^* - \alpha k_P r^* s, \\ d[RR]/dt &= k_P r r^* + k_E[SR] - k_D[RR], \\ d[SR]/dt &= \alpha k_P s^* r - k_E[SR], \end{aligned} \tag{5.2}$$

and the corresponding equations for s, s^*, $[SS]$, and $[RS]$ are similarly written. The total concentration of the R enantiomer is $r_t = r + r^* + 2[RR] + [SR] + [RS]$, and that of the S enantiomer is $s_t = s + s^* + 2[SS] + [SR] + [RS]$. Since the chirality conversion occurs only by epimerization and the total concentration $c = r_t + s_t$ is conserved, the chirality variation is given by

$$dr_t/dt = k_E([SR] - [RS]) = -ds_t/dt. \tag{5.3}$$

When the depolymerization and epimerization processes are very fast ($k_D, k_E \gg k_P c$), the dimer concentrations relax quickly to the steady state at which $d[SR]/dt = d[RR]/dt = 0$. The concentration of the heterodimer SR is determined

by the monomer concentrations as $[SR] = (\alpha k_P/k_E)s^* r$. Further, by assuming that polymerization is fast when compared to the external activation ($k_P c \gg k_A$), the concentrations of the activated enantiomers relax to the steady state at which $dr^*/dt = ds^*/dt = 0$ with a steady-state value $s^* = k_A s/k_P(\alpha r + s)$. Consequently, the heterodimer concentrations are determined as functions of the unactivated monomer concentrations r and s as

$$[SR] = \frac{k_A}{k_E}\frac{\alpha rs}{\alpha r + s}, \qquad [RS] = \frac{k_A}{k_E}\frac{\alpha rs}{r + \alpha s}. \tag{5.4}$$

The concentration $[RS]$ is obtained by substituting $r \leftrightarrow s$ in the formula for $[SR]$. The two heterodimers have different steady-state concentrations because the polymerization rate differs for homopolymers and heteropolymers; i.e., polymerization is chirality sensitive. In this quasisteady state where $k_D, k_E \gg k_P c \gg k_A$, the concentrations of the dimers and activated molecules are negligible when compared with that of the unactivated monomers. Then $dr_t/dt = dr/dt$ and the slow evolution of the unactivated monomer concentrations reduces to

$$\frac{dr}{dt} = \alpha k_A rs\left(\frac{1}{\alpha r + s} - \frac{1}{r + \alpha s}\right) = -\frac{ds}{dt}. \tag{5.5}$$

Since $0 < \alpha < 1$, the difference in Eq. (5.5) is positive when $r > s$. Thus the concentration of the majority enantiomer increases at the cost of the minority. Also, the chiral order parameter is written as $\phi = (r - s)/(r + s)$ with its evolution as

$$\frac{d\phi}{dt} = \frac{2\alpha(1-\alpha)}{(1+\alpha)^2 - (1-\alpha)^2\phi^2} k_A \phi(1 - \phi^2). \tag{5.6}$$

The evolution given by Eq. (5.6) is similar to Eq. (2.6) in the Frank model, to Eq. (3.2) for crystal growth, and to Eq. (4.7) for the Soai reaction. The racemic state with $\phi = 0$ is unstable, and homochirality with $|\phi| = 1$ is eventually achieved. Further, Eq. (5.6) shows that homochirality is induced by the external activation process of enantiomers, k_A.

VI. CONCLUSION AND DISCUSSION

We reviewed recent experimental and theoretical developments on chiral symmetry breaking to homochirality that occurred in the last two decades. The subject is multidisciplinary, and the studies span a wide range of fields including crystal growth, organic chemistry, and biochemistry. Various theoretical models for these systems have shown that the approach to homochirality is essentially described by the universal time evolution equation for the chiral order parameter ϕ, written as

$$\frac{d\phi}{dt} = A(t)\phi(1 - \phi^2). \tag{6.1}$$

From the symmetry point of view, this is the simplest form of evolution to homochirality. By including reverse or spontaneous production processes, it is modified to Eq. (2.7) and the system may eventually relax to a state with a broken chiral symmetry ($\phi \neq 0$) (Kondepudi and Nelson, 1985). A well-known example which leads to symmetry breaking is the time-dependent Ginzburg-Landau equation for the equilibrium phase transition. However, there is a great difference between the TDGL equation and Eq. (6.1). The present Eq. (6.1) is derived kinetically, whereas the TDGL equation is based on the minimization of the free energy involved. The coefficient A in Eq. (6.1) sometimes depends on time, reflecting that the systems that show homochirality are externally driven far from equilibrium.

Since the form of the nonlinear time evolution, as given by Eq. (6.1), is almost trivial if symmetry breaking occurs, a theory has to identify the mechanism that establishes nonlinearity for a specific system or a model. For the classical Frank model, mutual antagonism leads to nonlinearity (Frank, 1953). For crystal growth in solution under grinding, it is the mutual screening of active growth zones around the crystal periphery when two crystallites of opposite enantiomorphs come into proximity (Saito and Hyuga, 2010). The growth of both enantiomorphs is suppressed in a manner similar to the Frank model's mutual antagonism. In a chemical reaction, the origin of nonlinearity is an autocatalytic process mediated by homodimers that promote the production of enantiomers of their respective types (Blackmond *et al.*, 2001; Sato *et al.*, 2001). For the APED model of homochirality in life, nonlinearity is induced by chiroselective polymerization and epimerization processes (Plasson, Bersini, and Commeyras, 2004). The autocatalytic process is not necessary for this case.

Nonlinearity in the system is not sufficient to make the system homochiral. The coefficient A should not vanish. In both crystal growth and organic chemical systems, A is found to be proportional to the product of the concentrations of the achiral reactant and the total chiral products. In crystal growth, attrition or grinding constantly recycles the achiral reactant, and homochirality is established as shown in the experiment by Viedma (2005). In contrast, in the Soai chemical reaction, the reaction proceeds irreversibly and the achiral reactant is consumed to extinction. Therefore, even though the enantiomeric excess is amplified, homochirality cannot be achieved in this experiment (Soai *et al.*, 1995). In order to establish homochirality, one has to supply achiral reactants by recycling. This supply can be provided by an open steady flow (Saito and Hyuga, 2005b) or by chemical activation (Plasson, 2008). In the APED model for biomolecular systems, the depolymerization process recycles enantiomeric monomers. Here the coefficient A is independent of time but is proportional to the rate of external activation, thereby indicating that the system has to be driven externally away from equilibrium.

All these examples indicate that the system has to be driven out of equilibrium to maintain a finite value of the coefficient A. Recycling supplies achiral reactants or monomers that have higher free energy than the reaction products or grown crystals. In the APED model, free energy input is necessary to activate monomers to cause polymerization. Thus, an external supply of free energy to the system is required to maintain homochirality (Plasson and Brandenburg, 2010). Viedma and Cintas (2011) recently proposed another means to supply energy to the system. By thermally cycling the solution with d and l $NaClO_3$ crystals between hot and cool zones, the initial racemic mixture was found to be converted into a solid of single chirality. A similar thermal cycle was

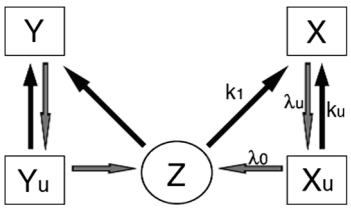

FIG. 21. Simplified Uwaha model of chiral crystal growth. From Uwaha, 2008.

successfully applied to replicate RNA (Krammer, Möller, and Braun, 2012).

We now consider other possibilities to achieve homochirality. Even though Eq. (6.1) is the simplest, it is by no means a unique equation to establish homochirality. For example, the model proposed by Uwaha (2004) for homochiral crystal growth yields another set of chirality evolution equations. He described the model in terms of mass fractions of chiral crystals x and y as well as those of chiral units x_u and y_u, and that of achiral molecules z, as shown in Fig. 21. Their evolution in a simplified case (McBride and Tully, 2008; Uwaha, 2008) can be easily transformed into those of two chiral order parameters $\phi = (x - y)/(x + y)$ and $\phi_u = (x_u - y_u)/(x_u + y_u)$ as

$$\frac{d\phi_u}{dt} = -k_u \frac{x+y}{2}\phi(1-\phi_u^2) + \lambda_u \frac{x+y}{x_u+y_u}(\phi - \phi_u),$$
$$\frac{d\phi}{dt} = k_u \frac{x_u+y_u}{2}\phi_u(1-\phi^2), \tag{6.2}$$

where k_u denotes the growth rate of chiral crystals by incorporating chiral units, and λ_u denotes the recycling rate of chiral units from chiral crystals. It is clear that there are racemic, i.e., $\phi = \phi_u = 0$, and homochiral, $\phi = \phi_u = \pm 1$, fixed points. As long as $\lambda_u > k_u(x_u + y_u)/2$, the racemic fixed point is linearly unstable, and homochirality is attained. There may be many other possibilities for the mechanism of homochirality in life, such as the polymerization models, and for the novel time evolution of chiral order parameters. Homochirality in life still remains a mystery, and further studies are required in this direction.

Thus far, we stressed the academic interest in homochirality; finally, we comment on the practical importance of the study of homochirality. Since living organisms are homochiral, two enantiomers react differently to living matter; it is possible that one enantiomer can be medically useful while the other might be harmful. Therefore, the control of the chirality of organic molecules at the production stage has practical and technological importance. The chirality of the product is usually controlled by chiral catalysts, but it may be useful if we can control chirality by external physical processes such as grinding or a thermal cycle.

ACKNOWLEDGMENTS

We are grateful to Christobal Viedma, Kenzo Soai, and Raphael Plasson for their valuable comments on the manuscript, and Masao Kitamura for providing us valuable references on quartz. Y. S. acknowledges the financial support provided by a Grant-in-Aid for Scientific Research, Grant No. 23540456, from the Japan Society for the Promotion of Science.

REFERENCES

Abrahams, S. C., and J. L. Bernstein, 1977, Acta Crystallogr. Sect. B **33**, 3601.
Arago, F., 1811, Mém. de la classe des sciences math. et phys. de l'Inst. **1**, 93.
Arago, F., 1858, OEuvres complètes de François Arago **10**, 36.
Avalos, M., R. Babiano, P. Cintas, H. Jiménez, and J. C. Palacios, 2000, Tetrahedron: Asymmetry **11**, 2845.
Avetisov, V., and V. Goldanskii, 1996, Proc. Natl. Acad. Sci. U.S.A. **93**, 11 435.
Bada, J. L., 1985, Annu. Rev. Earth Planet. Sci. **13**, 241.
Bada, J. L., 1995, Nature (London) **374**, 594.
Bailey, J., A. Chrysostomou, J. H. Hough, T. M. Gledhill, A. McCall, S. Clark, F. Mńard, and M. Tamura, 1998, Science **281**, 672.
Bakasov, A., T. Ha, and M. Quack, 1998, J. Chem. Phys. **109**, 7263.
Balavoine, G., A. Moradopour, and H. Kagan, 1974, J. Am. Chem. Soc. **96**, 5152.
Blackmond, D. G., 2004, Proc. Natl. Acad. Sci. U.S.A. **101**, 5732.
Blackmond, D. G., and O. K. Matar, 2008, J. Phys. Chem. B **112**, 5098.
Blackmond, D. G., C. R. McMillan, S. Ramdeehul, A. Shorm, and J. M. Brown, 2001, J. Am. Chem. Soc. **123**, 10 103.
Bonner, W. A., 1991, Origins Life Evol. Biosphere **21**, 59.
Bonner, W. A., 2000, Chirality **12**, 114.
Bonner, W. A., P. R. Kavasmaneck, F. S. Martin, and J. J. Flores, 1974, Science **186**, 143.
Brandenburg, A., A. C. Andersen, S. Höfner, and M. Nilsson, 2005, Origins Life Evol. Biosphere **35**, 225.
Brandenburg, A., H. J. Lehto, and K. M. Lehto, 2007, Astrobiology **7**, 725.
Buhse, T., 2003, Tetrahedron: Asymmetry **14**, 1055.
Buhse, T., D. Durand, D. Kondepudi, J. Laudadio, and S. Spilker, 2000, Phys. Rev. Lett. **84**, 4405.
Calvin, M., 1969, *Chemical Evolution* (Oxford University Press, Oxford).
Cartwright, J. H. E., J. M. Garcia-Ruiz, O. Piro, C. I. Sainz-Diaz, and I. Tuval, 2004, Phys. Rev. Lett. **93**, 035502.
Cartwright, J. H. E., O. Piro, and I. Tuval, 2007, Phys. Rev. Lett. **98**, 165501.
Cronin, J. R., and S. Pizzarello, 1997, Science **275**, 951.
Dana, E. S., 1915, *The System of Mineralogy of James Dwight Dana 1837–1868: Descriptive Mineralogy.* (Wiley, New York), 6th ed.
Engel, M. H., and S. A. Macko, 1997, Nature (London) **389**, 265.
Ercolani, G., and L. Schiaffino, 2011, J. Org. Chem. **76**, 2619.
Feringa, B. L., and R. A. van Delden, 1999, Angew. Chem., Int. Ed. **38**, 3418.
Frank, F. C., 1953, Biochim. Biophys. Acta **11**, 459.
Frondel, C., 1978, Am. Mineral. **63**, 17.
Gilbert, W., 1986, Nature (London) **319**, 618.
Girard, C., and H. B. Kagan, 1998, Angew. Chem., Int. Ed. **37**, 2922.
Goldanskii, V. I., and V. V. Kuz'min, 1988, Z. Phys. Chem. (Leipzig) **269**, 216.
Gridnev, I. D., 2006, Chem. Lett. **35**, 148.
Gridnev, I. D., and J. M. Brown, 2004, Proc. Natl. Acad. Sci. U.S.A. **101**, 5727.
Gridnev, I. D., J. M. Serafimov, H. Quiney, and J. M. Brown, 2003, Org. Biomol. Chem. **1**, 3811.
Guerrier-Takada, C., K. G. A. Marsh, N. Pace, and S. Altman, 1983, Cell **35**, 849.
Islas, J. R., D. Lavabre, J.-M. Grevy, R. H. Lamoneda, H. R. Cabrera, J.-C. Micheau, and T. Buhse, 2005, Proc. Natl. Acad. Sci. U.S.A. **102**, 13 743.

Japp, F. R., 1898, Nature (London) **58**, 452.
Joyce, G. F., G. M. Visser, C. A. A. van Boeckel, J. H. van Boom, L. E. Orgel, and J. Westrenen, 1984, Nature (London) **310**, 602.
Kagan, H., G. Balvoine, and A. Moradpour, 1974, J. Mol. Evol. **4**, 41.
Kawasaki, T., Y. Matsumura, T. Tsutsumi, K. Suzuki, M. Ito, and K. Soai, 2009, Science **324**, 492.
Kawasaki, T., M. Sato, S. Ishiguro, T. Saito, Y. Morishita, I. Sato, H. Nishino, Y. Inoue, and K. Soai, 2005, J. Am. Chem. Soc. **127**, 3274.
Kawasaki, T., K. Suzuki, M. Shimizu, K. Ishikawa, and K. Soai, 2006, Chirality **18**, 479.
Lord Kelvin, 1904, *Baltimore Lectures on Molecular Dynamics and the Wave Theory of Light* (C. J. Clay and Sons, London).
Kipping, F. S., and W. J. Pope, 1898a, J. Chem. Soc. Trans. **73**, 606.
Kipping, F. S., and W. J. Pope, 1898b, Nature (London) **59**, 53.
Klabunovskii, E. I., and W. Thiemann, 2000, Origins Life Evol. Biosphere **30**, 431.
Kondepudi, D. K., and K. Asakura, 2001, Acc. Chem. Res. **34**, 946.
Kondepudi, D. K., K. L. Bullock, J. A. Digits, J. K. Hall, and J. M. Miller, 1993, J. Am. Chem. Soc. **115**, 10 211.
Kondepudi, D. K., R. J. Kaufman, and N. Singh, 1990, Science **250**, 975.
Kondepudi, D. K., J. Laudadio, and K. Asakura, 1999, J. Am. Chem. Soc. **121**, 1448.
Kondepudi, D. K., and G. W. Nelson, 1983, Phys. Rev. Lett. **50**, 1023.
Kondepudi, D. K., and G. W. Nelson, 1985, Nature (London) **314**, 438.
Kovacs, K. I., I. Keszthelyi, and V. J. Goldanskii, 1981, Origins of Life **11**, 93.
Krammer, H., F. M. Möller, and D. Braun, 2012, Phys. Rev. Lett. **108**, 238104.
Kriausakul, N., and R. M. Mitterer, 1978, Science **201**, 1011.
Kruger, K., P. J. Grabowski, J. Sands, D. E. Gottschling, and T. R. Cech, 1982, Cell **31**, 147.
Kuhn, W., and E. Braun, 1929, Naturwissenschaften **17**, 227.
Kuhn, W., and E. Knopf, 1930, Naturwissenschaften **18**, 183.
Lee, T. D., and C. N. Yang, 1956, Phys. Rev. **104**, 254.
Lente, G., 2004, J. Phys. Chem. A **108**, 9475.
Lente, G., 2005, J. Phys. Chem. A **109**, 11 058.
Lente, G., 2006, J. Phys. Chem. A **110**, 12 711.
Lente, G., 2007, Phys. Chem. Chem. Phys. **9**, 6134.
Martin, B., A. Tharrington, and X. l. Wu, 1996, Phys. Rev. Lett. **77**, 2826.
Mason, S. F., and G. E. Tranter, 1985, Proc. R. Soc. A **397**, 45.
McBride, J. M., and R. L. Carter, 1991, Angew. Chem., Int. Ed. Engl. **30**, 293.
McBride, J. M., and J. C. Tully, 2008, Nature (London) **452**, 161.
Metcalfe, G., and J. M. Ottino, 1994, Phys. Rev. Lett. **72**, 2875.
Milton, R. C., S. C. Milton, and S. B. Kent, 1992, Science **256**, 1445.
Nelson, K. E., M. Levy, and S. L. Miller, 2000, Proc. Natl. Acad. Sci. U.S.A. **97**, 3868.
Nilsson, M., A. Brandenburg, A. C. Andersen, and S. Höfner, 2005, Int. J. Astrobiol. **4**, 233.
Noorduin, W. L., T. Izumi, A. Milemaggi, M. Leeman, H. Meekes, W. J. P. V. Enckevort, R. M. Kellog, B. Kaptein, E. Vleg, and D. G. Blackmond, 2008, J. Am. Chem. Soc. **130**, 1158.
Noorduin, W. L., H. Meeks, A. A. C. Bode, W. J. P. V. Enckvort, B. Kapstein, R. M. Kellog, and E. Vleg, 2008, Cryst. Growth Des. **8**, 1675.
Orgel, L. E., 2004, Crit. Rev. Biochem. Mol. Biol. **39**, 99.
Pasteur, M. L., 1848a, Comptes Rendus **26**, 535.
Pasteur, M. L., 1848b, Ann. Chim. Phys. **24**, 442.
Pasteur, M. L., 1875, Comptes Rendus **81**, 128.
Pearson, K., 1898a, Nature (London) **58**, 495.
Pearson, K., 1898b, Nature (London) **59**, 30.
Plasson, R., 2008, J. Phys. Chem. B **112**, 9550.
Plasson, R., H. Bersini, and A. Commeyras, 2004, Proc. Natl. Acad. Sci. U.S.A. **101**, 16 733.
Plasson, R., and A. Brandenburg, 2010, Origins Life Evol. Biosphere **40**, 93.
Plasson, R., D. K. Kondepudi, H. Bersini, A. Commeyras, and K. Asakura, 2007, Chirality **19**, 589.
Saito, Y., and H. Hyuga, 2004, J. Phys. Soc. Jpn. **73**, 33.
Saito, Y., and H. Hyuga, 2005a, J. Phys. Soc. Jpn. **74**, 535.
Saito, Y., and H. Hyuga, 2005b, J. Phys. Soc. Jpn. **74**, 1629.
Saito, Y., and H. Hyuga, 2008, J. Phys. Soc. Jpn. **77**, 113001.
Saito, Y., and H. Hyuga, 2009, J. Phys. Soc. Jpn. **78**, 104001.
Saito, Y., and H. Hyuga, 2010, J. Phys. Soc. Jpn. **79**, 083002.
Saito, Y., and H. Hyuga, 2011, J. Cryst. Growth **318**, 93.
Saito, Y., T. Sugimori, and H. Hyuga, 2007, J. Phys. Soc. Jpn. **76**, 044802.
Sandars, P. G. H., 2003, Origins Life Evol. Biosphere **33**, 575.
Sato, I., K. Kadowaki, and K. Soai, 2000, Angew. Chem., Int. Ed. **39**, 1510.
Sato, I., D. Omiya, H. Igarashi, K. Kato, Y. Ogi, K. Tsukiyama, and K. Soai, 2003, Tetrahedron: Asymmetry **14**, 975.
Sato, I., D. Omiya, K. Tsukiyama, Y. Ogi, and K. Soai, 2001, Tetrahedron: Asymmetry **12**, 1965.
Sato, I., H. Urabe, S. Ishiguro, K. T. Shibata, and K. Soai, 2003, Angew. Chem., Int. Ed. **42**, 315.
Schoning, K., P. Scholz, S. Guntha, X. Wu, R. Krishunamurthy, and A. Eschenmoser, 2000, Science **290**, 1347.
Siegel, J. S., 1998, Chirality **10**, 24.
Singleton, D. A., and L. K. Vo, 2002, J. Am. Chem. Soc. **124**, 10 010.
Singleton, D. A., and L. K. Vo, 2003, Org. Lett. **5**, 4337.
Soai, K., S. Osanai, K. Kadowaki, S. Yonekubo, T. Shibata, and I. Sato, 1999, J. Am. Chem. Soc. **121**, 11 235.
Soai, K., *et al.*, 2003, Tetrahedron: Asymmetry **14**, 185.
Soai, K., T. Shibata, H. Morioka, and K. Choji, 1995, Nature (London) **378**, 767.
Tsogoeva, S. B., S. Wei, M. Freund, and M. Mauksch, 2009, Angew. Chem., Int. Ed. **48**, 590.
Uwaha, M., 2004, J. Phys. Soc. Jpn. **73**, 2601.
Uwaha, M., 2008, J. Phys. Soc. Jpn. **77**, 083802.
Viedma, C., 2005, Phys. Rev. Lett. **94**, 065504.
Viedma, C., and P. Cintas, 2011, Chem. Commun. (Cambridge) **47**, 12 786.
Viedma, C., J. E. Ortiz, T. de Torres, T. Izumi, and D. G. Blackmond, 2008, J. Am. Chem. Soc. **130**, 15 274.
Wesendrup, R., J. K. Laerdahl, R. N. Compton, and P. Schwerdtfeger, 2003, J. Phys. Chem. A **107**, 6668.
Wu, C. S., E. Ambler, R. W. Hayward, D. D. Hoppes, and R. P. Hudson, 1957, Phys. Rev. **105**, 1413.
Yamagata, Y., 1966, J. Theor. Biol. **11**, 495.